1-1-2008

Characterization of RQ1, a mutant involved in nervous system development in C. Elegans

Matthew M. Bueno de Mesquita
Ryerson University

CHARACTERIZATION OF *RQ1*, A MUTANT INVOLVED IN NERVOUS SYSTEM DEVELOPMENT IN *C. ELEGANS*

By

Matthew M. Bueno de Mesquita

BSc., Applied Chemistry and Biology, Ryerson University, 2006

A thesis

presented to Ryerson University

in partial fulfillment of the

requirements for the degree of

Masters of Sciences

in the Program of

Molecular Science

Toronto, Ontario, Canada, 2008

I hereby declare that I am the sole author of this thesis or dissertation.

I authorize Ryerson University to lend this thesis or dissertation to other institutions or individuals for the purpose of scholarly research.

Matthew M. Bueno de Mesquita

I further authorize Ryerson University to reproduce this thesis or dissertation by photocopying or by other means, in total or in part, at the request of other institutions or individuals for the purpose of scholarly research.

Matthew M. Bueno de Mesquita

Characterization of *rq1*, a mutant involved in nervous system development in *C. elegans*. MSc. 2008. Matthew Bueno de Mesquita, Molecular Science, Ryerson University.

Abstract

During the development of the nervous system, guidance cues provide directional information to the growth cones of migrating axons. In *C. elegans,* ventral to dorsal migration is in part mediated by the ligand UNC-6 and its receptor UNC-5. In an UNC-5 null mutant the DA and DB motor neuron axons fail to migrate in a wild type manner to the dorsal cord, despite initial dorsalward outgrowth from the cell bodies. A genetic enhancer screen was conducted in an UNC-5 null strain and one mutant, *rq1*, was found to have increased axon guidance defects. To identify the mutated gene in *rq1*, microinjection experiments were performed and were able to rescue two *rq1* phenotypes. RNAi experiments were performed where double stranded RNA corresponding to all the genes in the region were used individually to knock out the transcripts. Several of these were able to phenocopy the defects of *rq1*. The *rq1* mutation could be located in any one of five genes known to be present on the rescuing cosmid while combined results implicate three strong candidate genes, M03C11.8, H04D03.1 and H04D03.4.

Acknowledgments

I would like to thank my supervisor Dr. Marie Killeen for her guidance and leadership. The research of Stephanie Sybingco which yielded the *rq1* mutant was the basis for all of the research performed in this thesis. Sang-Hyeon Park spent many hours peering through a microscope that were required to generate the data on the enhancement of the axon guidance phenotypes in the mutant background. The experiments in this thesis could not have been performed without Ghanna Kholkina, her contributions can not be understated. The laboratory would not run in the summers with out the help of Viktoria Serdetchnaia. Zafar Naqvi, a fellow graduate student who hit the ground running, has been instrumental in more ways than I have space to list.

At Mount Sinai Hospital, I would like to thank Dr. Joseph Culotti and his lab for their expertise, guidance and continued support, especially Lijia Zhang for all of her microinjection, training, troubleshooting and advice. I would also like to thank Dr. Wendy Johnston for her analysis of the *rq1* embryos and her guidance.

Great appreciation needs to be extended to my family and in particular all of my grandparental units who have been the enablers in my research endeavors. To Robyn who kept me sane for two years, thank you.

Table of Contents

List of Figures

List of Tables

List of Abbreviations

AMP	Adenosine mono-phosphate
AP	anterior-posterior
BLAST	Basic Local Alignment Search Tool
DCC	deleted in colorectal cancer
DD	Death domain
DNA	deoxyribonucleic acid
dsRNA	Double-stranded ribonucleic acid
Dpy	Dumpy
DTC	distal tip cell
DV	dorsal-ventral
Fgf	Fibroblast growth factors
EMB	embryonic lethal
EMS	ethyl methylsulfonate; ethyl methanesulfonate
GABA	gamma-aminobutyric acid
GFP	green fluorescent protein
Ig	Immunoglobulin
JM	Juxta membrane
MCS	multiple cloning site
mM	Millimolar
NGM	Nematode growth media
PCR	polymerase chain reaction
PICK	C-kinase-1
PKC	Protein Kinase C
Rcm	rostral cerebellar malformation
RE	Restriction endonuclease
Robo	Roundabout
RNAi	ribonucleic acid interference
Shh	Sonic hedgehog
Smo	Smoothened
SNF	Sucrose non-fermentor
SNP	single nucleotide polymorphism
TGF-β	transforming growth factor β
TM	Transmembrane
TRPC	transient receptor potential channels
Tsp	Thrombospondin type 1
µl	Microliter
UNC	Uncoordinated
Wnt	Wingless/int

1 Introduction

The nervous system has been the subject of intensive research since scientists were first able to observe it. Santiago Ramon y Cajal, arguably the father of modern neurology, described neurons as being polar cells which make up a vast network of interconnectivity (Cajal, 1890). Since then, great efforts have been made in order to understand how the nervous system develops its complex web of neuronal connections. It has been estimated that the human brain contains 10×10^{12} neurons and it is nearly impossible to study individual neurons in such a complex milieu. For this reason, much use has been made of organisms with more simple nervous systems such as the nematode *Caenorhabditis elegans* (*C. elegans)* and the fruit-fly, *Drosophila melanogaster.* In these organisms neurons can be tagged and visualized using fluorescent reporter genes in specific groups or individually. The work described in this thesis uses the model organism *C. elegans* to study ventral to dorsal motor axon guidance.

1.1 Detailed Overview of Ligand/Receptor Mediated Axon Guidance

The nervous system in higher organisms such as humans is highly conserved amongst many species. Much of our understanding of the cues and receptors involved in the development of the mammalian nervous system has been a direct result of research in model organisms such as *Drosophila* and *C. elegans*. The mechanisms of pioneer axon guidance are not completely elucidated. They can, at present, be attributed to a combination of pathways that depend on ligand expression and the expression of their

receptors at particular times and places during development. These pathways are set up by the expression of ligands at specific locations at specific stages of development which have been proposed to create concentration gradients across the developing animal. When the specialized receptors for these ligands bind their target, they cause downstream internal cytoskeletal restructuring which ultimately leads to either an attractive or a repulsive response to the localized concentration of expressed ligand. There are five major ligands involved in nervous system development and they are Netrin/UNC-6, Slit/Slt-1, semaphorins, ephrins and Wnt (Chilton, 2006; Colavita et al., 1998; Blelloch et al., 1999) These are depicted in Figure 1.1. Sonic hedgehog, FGFs and TGF-beta/*unc-129* also play roles in nervous system development.

The ligand UNC-6/Netrin is involved in many developmental processes. It was first found in *C. elegans,* (Ishii et al., 1992) where it is primarily involved in dorsal-ventral developmental events such as pioneer axon guidance. UNC-6 has homologues in many other organisms including humans (Moore et al., 2007). UNC-6/Netrin has two receptors, UNC-5 and UNC-40 in *C. elegans* (Chan et al., 1996; Leung-Hagesteijn et al., 1992). This system is the focus of this thesis and will be discussed in depth in the sections to follow.

Semaphorins are divided into classes one through eight with the third class being primarily involved in growth cone collapse (Chilton, 2006). There are two receptor families for semaphorins which are neuropilins and plexins (Chilton, 2006). Between these two receptor families there is a complicated relationship. This is evident in the fact that plexins do not bind class 3 semaphorins while neuropilins do not bind class 4 or class 7 semaphorin, yet neuropilins and plexins can come together to form receptor complexes for other classes of semaphorins (Chilton, 2006). The intricacies of semaphorins and their highly specific interactions with neuropilins and plexins will not be discussed further as it is not critical to the focus of this thesis.

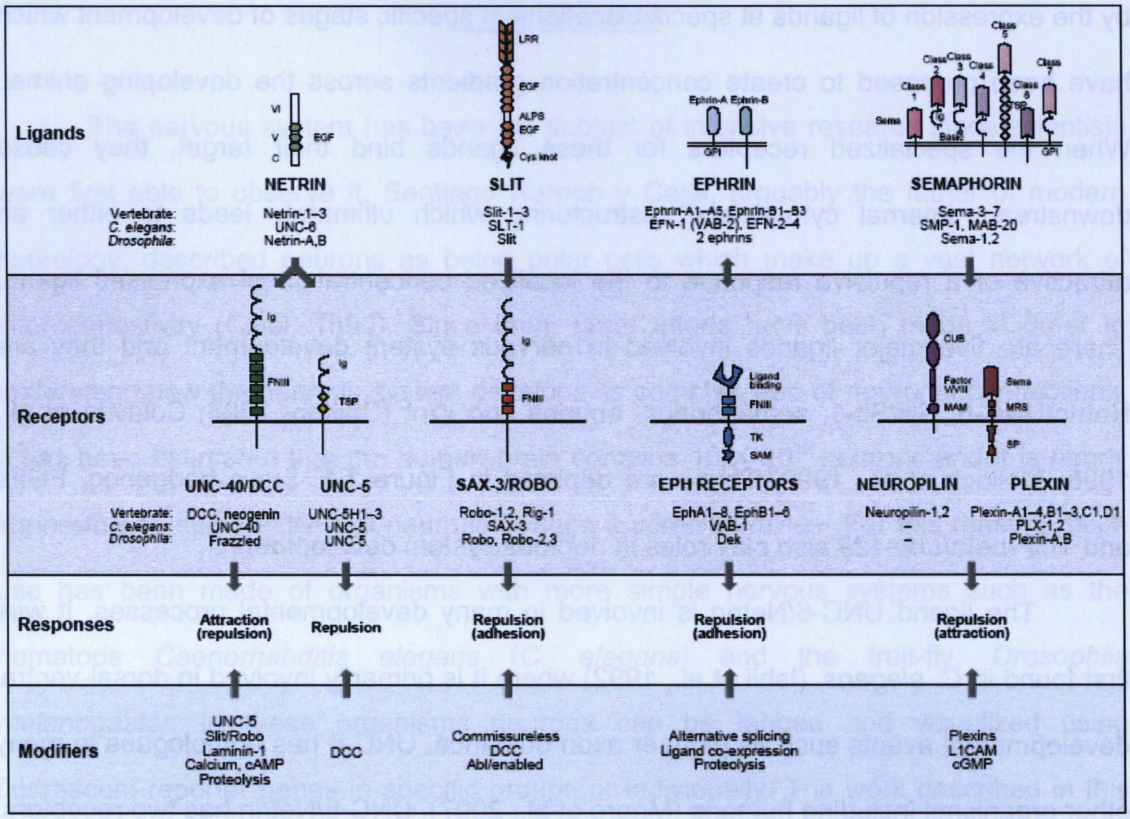

Figure 1.1: Axon guidance ligands and their receptors

The diagram shows a summary of four of the main guidance cues and receptors found in axon guidance in *C. elegans*, adapted from Figure one of Yu and Bargmann (2001).

Ephrins are a family of ligands with their receptors appropriately named the Eph receptors. The ligands as well as their receptors are divided into two classes, A and B. The EphrinA and EphrinB classes bind the EphA and EphB receptors respectively. It has been demonstrated that in chick retina the A class is involved in anterior-posterior guidance and the B class is involved in dorsal-ventral guidance (Chilton, 2006).

Slit, originally identified in *Drosophila* (Rothberg et al., 1988), and its *C. elegans* homologue SLT-1 (Hao et al., 2001) are primarily involved in dorsal-ventral axon guidance. In humans there are three homologues of Slit involved in neuronal development (Itoh et al., 1998). SLT-1 is expressed dorsally in *C. elegans* and in conjunction with its receptor, SAX-3 and in *Drosophila* Robo, can guide a migrating axon away from a SLT-1/Slit source (Hao et al., 2001). Recently, a second receptor for SLT-1 has been discovered in *C. elegans*, namely EVA-1 (Fujisawa et al., 2007). SLT-1/Slit is also involved in midline crossing in conjunction with the UNC-6/netrin pathway (Kidd et al., 1999).

The Wnt family of ligands plays many vital roles in development. Wnt/beta-catenin, for example, can function through *Frizzled* and *Disheveled* to regulate gene expression during cell fate as well as through *Disheveled* and Rho GTPases to regulate microtubule dynamics in *Drosophila* (Lu and Van Vactor, 2007). Also in *Drosophila,* Wnt signaling through *Ryk* and *Derailed* leads a migrating axon to be repulsed away from a Wnt source (Lu and Van Vactor, 2007). The *C. elegans* homologues of Wnt are *lin-44, egl-20 cwn-1, cwn-2 and mom-2,* while their receptors are *Frizzled/lin-17/mig-1, cfz-1, mom-5, Ryk/lin-18* and *Disheveled/dsh-1*. In *C. elegans,* several of the Wnt family of proteins are expressed in the posterior of the animal and create a concentration gradient anteriorly. Of the five Wnt family proteins CWN-1, CWN-2, LIN-44 and EGL-20 are all

expressed in the extreme posterior region during the early larval stages (Gleason et al., 2006; Pan et al., 2006) .

Sonic hedgehog (Shh) was originally described in *Drosophila* as acting with its mediator Smoothened (Smo) as a midline attractive cue for migrating axons (Charron et al., 2003; Erskine and Herrera, 2007). This was demonstrated *in vitro* by positioning Shh expressing COS cells beside rat E11 whole spinal cord explants and observing whether or not the migration of axons was affected by the gradient of Shh excreted by the COS cells. In this experiment, Shh was shown to be a chemo-attractant and in a similar experiment using rat spinal cord explants which did not express Smo, it was shown that Smo is required for Shh's chemo-attractive abilities (Charron et al., 2003).

Fibroblast growth factors (FGFs), like other developmentally expressed ligands, do not have fully elucidated roles in developmental processes. In a recent review, FGF and its receptor *Fgfr1* is described as an independent guidance pathway involved in mammalian forebrain commissures crossing the midline during development (Lindwall et al., 2007).

Transforming growth factor beta (TGF-beta) and its *C. elegans* homologue *unc-129* is expressed dorsally in the developing nematode and is required for motor axon guidance in the dorsal-ventral direction (Colavita et al., 1998). It was shown in *C. elegans* that *unc-129* is required for proper guidance of the DA/DB motor axons as demonstrated by the observed defects in an *unc-129* null allele. Since UNC-129 does not interact with any of the known TGF-beta family receptors it is hypothesized that UNC-129 either interacts with UNC-5 to regulate sensitivity in the UNC-6/Netrin pathway or that UNC-129 may participate in a separate signaling pathway (Colavita et al., 1998). The localization of guidance cue expression in *C. elegans* is depicted in Figure 1.2.

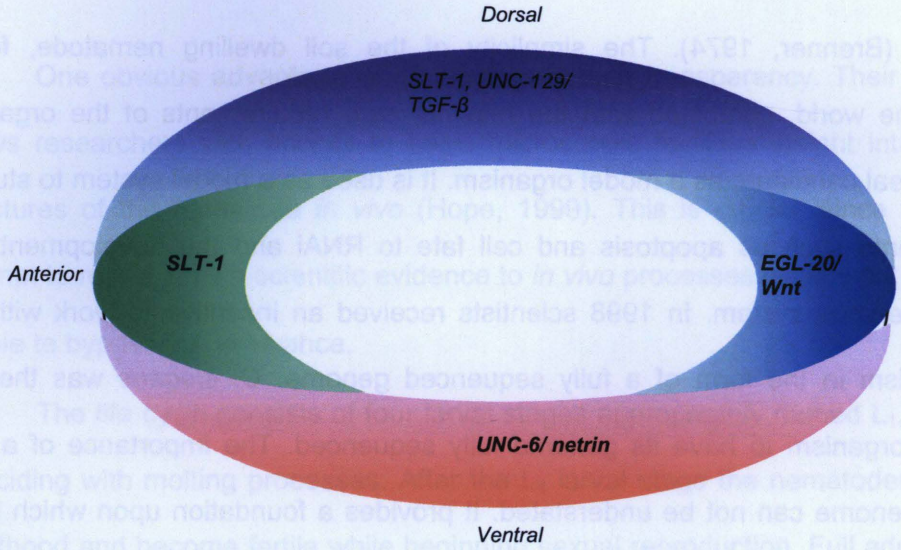

Figure 1.2: Localization of guidance cue expression in *C. elegans*

Expression and establishment of concentration gradients of the major *C. elegans* guidance cues. Adapted from Figure 2 of Blelloch *et al.* (1999)

1.2 *C. elegans* as a Model Organism

Caenorhabditis elegans was popularized as a model organism by Nobel laureate Dr. Brenner (Brenner, 1974). The simplicity of the soil dwelling nematode, found throughout the world, combined with the minimal care requirements of the organism made it an ideal candidate as a model organism. It is used as a model system to study a range of events such as apoptosis and cell fate to RNAi and the development and function of nervous system. In 1998 scientists received an incentive to work with the model organism in the form of a fully sequenced genome. *C. elegans* was the first multicellular organism to have its genome fully sequenced. The importance of a fully sequenced genome can not be understated. It provides a foundation upon which large bodies of scientific evidence can be built. With the more recent completion of the human genome, and even more recent completion of Dr. Craig Venter's genome, the genetic discoveries made in *C. elegans* become even more relevant due to its homology with humans.

C. elegans are nematodes of approximately one millimeter in length and are barely visible at full adulthood with the naked eye. They are temperature sensitive with a decreased generation time at higher temperatures while lower temperatures retard their progression to adulthood. At 20°C the generation time is three days from embryo to reproductive viability. A population of *C. elegans* consists mainly of hermaphrodites with males making up 0.02% of the population (Brenner, 1974). They are diploid eukaryotes with six chromosomes named by the roman numerals I through V as well as a sex chromosome called X and the entire genome is approximately 100Mbp and is predicted to contain just under 20,000 genes (Riddle et al., 1997). Their hermaphroditic reproduction makes them ideal as a genetic model organism. A sole parent allows recessive genetic lines to be carried indefinitely. Their relatively short generation time

lends itself well to classical genetic manipulations since large homozygous populations can be cultured easily. A diagrammatic representation of *C. elegans* is shown in Figure 1.3.

One obvious advantage of *C. elegans* is their transparency. Their transparency allows researchers with access to basic microscopic facilities insight into the internal structures of the nematode *in vivo* (Hope, 1999). This is crucial, since many studies attempt to relate *in vitro* scientific evidence to *in vivo* processes while work in *C. elegans* is able to bypass this hindrance.

The life cycle consists of four larval stages appropriately named L_1, L_2, L_3 and L_4 coinciding with molting processes. After the L_4 larval stage the nematodes enter young adulthood and become fertile while beginning sexual reproduction. Full adult nematodes can live for several days, and up to a week at optimal conditions. When confronted with starvation, *C. elegans* have the ability to alter their life cycle. Instead of progressing from L_2 to L_3, when faced with starvation, they proceed to the Dauer larval stage from the L_2 stage. A Dauer larval nematode can survive in adverse starvation conditions for up to four months. If conditions improve, Dauer larval *C. elegans* bypass the L_3 larval stage and progress directly to L_4 from which a normal progression to adulthood is followed (Jorgensen and Mango, 2002).

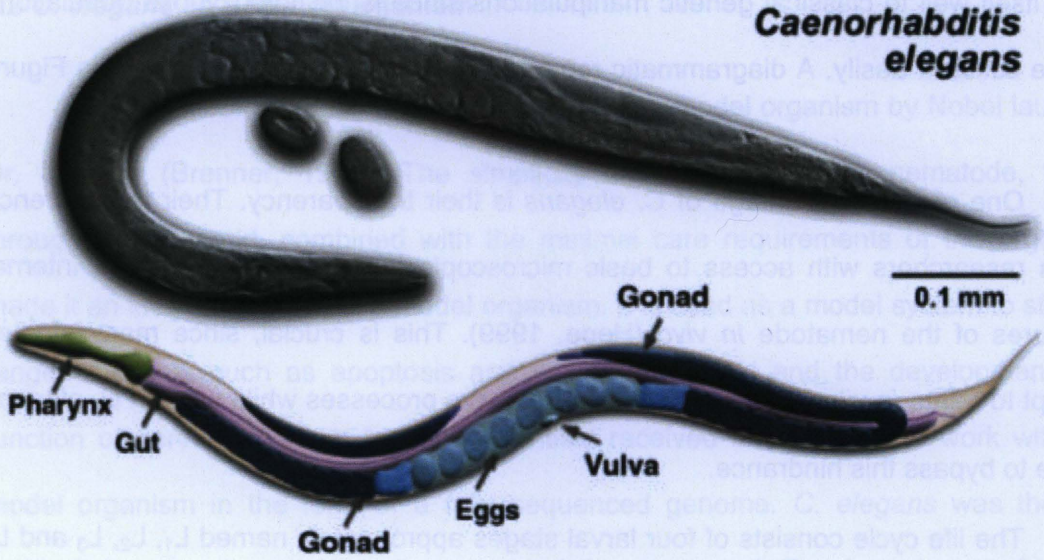

Figure 1.3: The *C. elegans* model organism

The gross morphology as well as internal structures of *C. elegans* is clearly visualized due to the transparent nature of the nematode. Figure adapted from Asahina et al. (2006).

1.3 Development of the *C. elegans* Nervous System

There are three main structures of the nervous system located throughout the body of the nematode. The nerve ring is located at the head of the animal around the pharynx. The ventral nerve cord runs along the ventral midline of the animal and dorsal nerve cord mirrors the ventral nerve cord running along the dorsal midline of the animal (White et al., 1986). The ventral and dorsal cords are located between the epidermis and the basal lamina of the epidermis. The epidermal basal lamina is required to compartmentalize the nerve cords and their projected axons between the epidermis and the interior mesoderm and musculature (Hedgecock et al., 1990). The focus will remain primarily on motor neurons that originate at the ventral nerve cord.

Wild type (N2) hermaphrodite *C. elegans* have a total of 302 neurons of 118 distinct different types. These groups are made up of neurons that have the same morphology but different locations throughout the body of the nematode (White et al., 1986). There are several classes of neurons, grouped according to their function. The classes are sensory, mechanosensory, motor neurons and the interneurons. The sensory group of neurons is responsible for the nematode's chemosensory abilities. The mechanosensory group of neurons is responsible for the nematode's ability to sense applied pressure. The motor neurons are responsible for controlling the musculature of the animal and the interneuron group makes up for the various levels of interconnectivity (White et al., 1986). There are thirty classes of motor neurons of which only eight originate from cell bodies along the ventral nerve cord. Four of the eight are associated with the ventral muscles, VA, VB, VD and VC, while the other four are associated with the dorsal muscles, DA, DB, DD and AS (White et al., 1986). Most develop post-embryonically, the exceptions are the DA and DB motor neurons which develop during embryonic stages. The DA and DB motor neurons communicate with their post-synaptic

partners by release of the neurotransmitter acetylcholine while other motor neurons including the VD and DD motor neurons use gamma-aminobuteric acid as their neurotransmitter (White et al., 1986). The nervous system structure is shown in Figure 1.4.

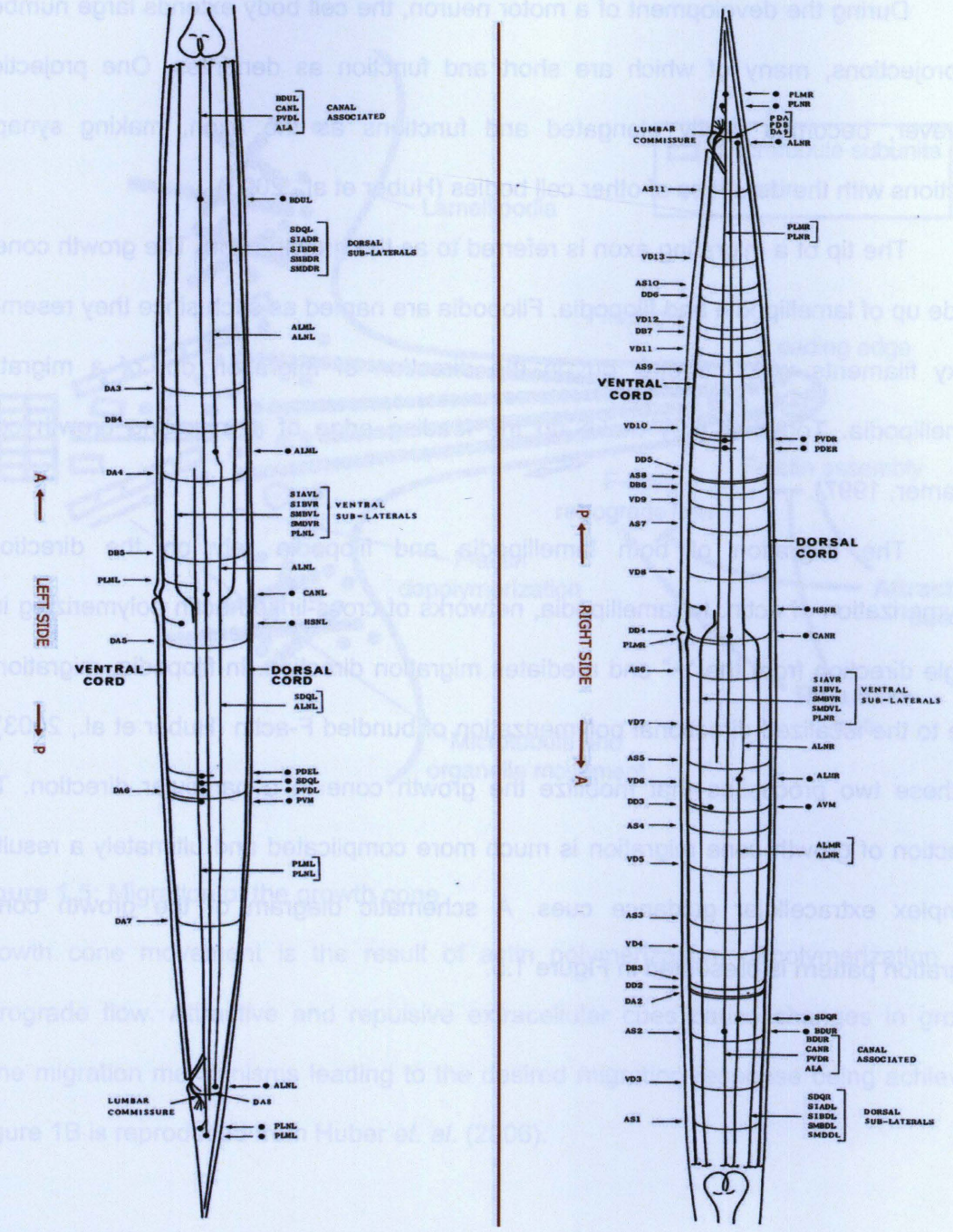

Figure 1.4: Diagram of wild type motor neuron patterning

The ventral and dorsal cords are located along the ventral and dorsal midlines respectively. Figure 7 reproduced from (White et al., 1986).

During the development of a motor neuron, the cell body extends large numbers of projections, many of which are short and function as dendrites. One projection, however, becomes vastly elongated and functions as the axon, making synaptic junctions with the dendrites of other cell bodies (Huber et al., 2003).

The tip of a migrating axon is referred to as the growth cone. The growth cone is made up of lamellipodia and filopodia. Filopodia are named as such since they resemble spiky filaments which stretch out in the direction of migration out of a migrating llamellipodia. Together they make up the leading edge of a migrating growth cone (Cramer, 1997).

The migration of both lamellipodia and filopodia rely on the directional polymerization of actin. In lamellipodia, networks of cross-linked actin polymerizing in a single direction from the "+" end mediates migration direction. In filopodia, migration is due to the localized directional polymerization of bundled F-actin (Huber et al., 2003). It is these two processes that mobilize the growth cone in a particular direction. The direction of growth cone migration is much more complicated and ultimately a result of complex extracellular guidance cues. A schematic diagram of the growth cone's migration pattern is presented in Figure 1.5.

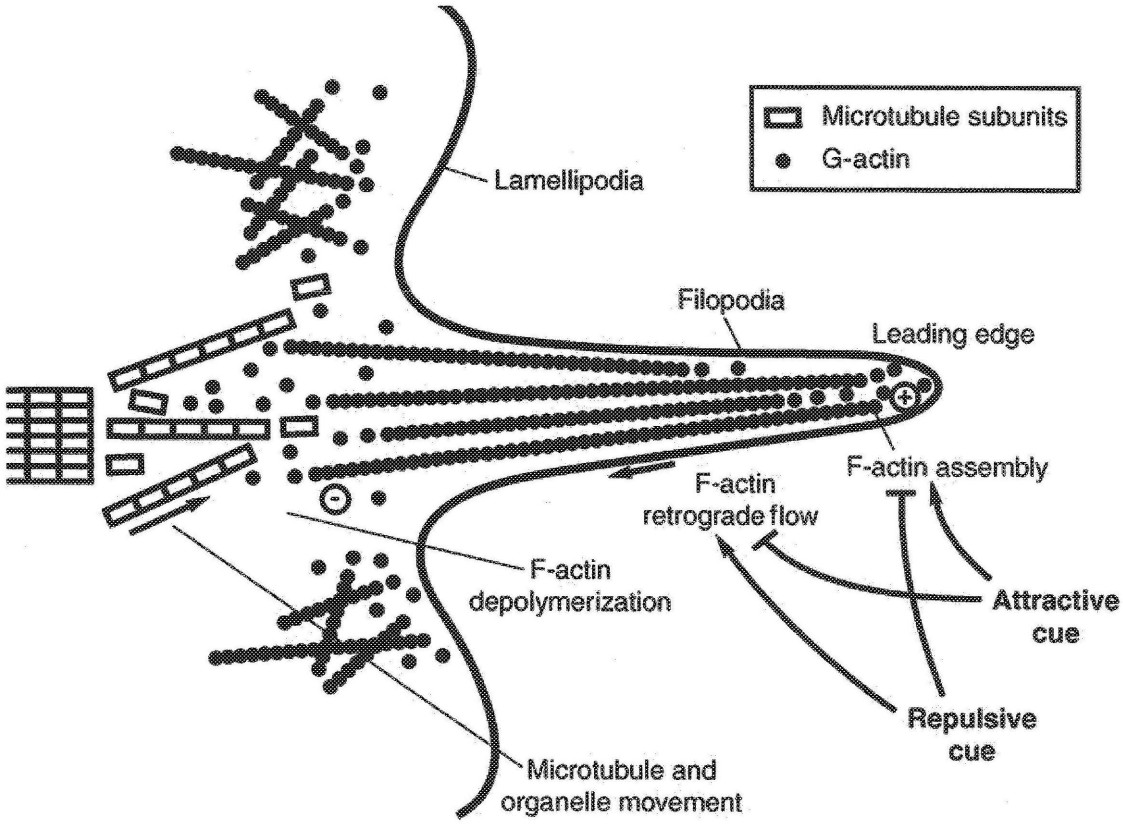

Figure 1.5: Migration of the growth cone

Growth cone movement is the result of actin polymerization, depolymerization and retrograde flow. Attractive and repulsive extracellular cues cause changes in growth cone migration mechanisms leading to the desired migration response being achieved. Figure 1B is reproduced from Huber *et. al.* (2006).

1.4. The UNC-6/Netrin System

C. elegans UNC-6 is a laminin-like molecule (Ishii et al., 1992) which serves as a bifunctional guidance cue for dorsal-ventral migration. Netrin/UNC-6 is a ligand secreted ventrally along the midline of the animal (Wadsworth et al., 1996). The localized expression sets up a ventral to dorsal concentration gradient of the ligand (Figure 1. 7). There are two single pass transmembrane receptors for UNC-6 in *C. elegans* which are UNC-5 and UNC-40 (Chan et al., 1996; Leung-Hagesteijn et al., 1992). Expression of UNC-40 alone on the growth cone of a migrating axon causes attraction to an UNC-6 source while expression of UNC-5, alone or in the presence of UNC-40, causes repulsion from an UNC-6 source (Merz and Culotti, 2000). A diagram illustrating the UNC-6/netrin system is presented in Figure 1.6.

Netrin is the vertebrate homologue of UNC-6 (Colamarino and Tessier-Lavigne, 1995; Serafini et al., 1996). Homologues of UNC-40 are Frazzled in *D. melanogaster* and DCC (Deleted in Colorectal Cancer) in vertebrates (Culotti and Merz, 1998). Homologues of UNC-5 are also called UNC-5 in many other systems since the protein was first identified in *C. elegans*, however, in vertebrates Rostral cerebellar malformation (Rcm) is used interchangably (Ackerman et al., 1997). In many higher organisms several homologues of the *C. elegans* UNC-5 are present. For example, in humans there are UNC-5 versions A through D (Leonardo et al., 1997; Round and Stein, 2007).

The role of the netrin pathway proteins in growth cone migration along with a schematic of UNC-6/netrin is presented in Figure 1.7. The interaction of UNC-40 with UNC-5 is ligand-dependent and it has been demonstrated that UNC5H2 co-precipitated with DCC from COS-1 cells only in the presence of netrin-1 (Hong et al., 2000). They also showed that UNC-5H2 residues 707-724 are required for proper function and thus this domain is named DB for its requirement in binding DCC.

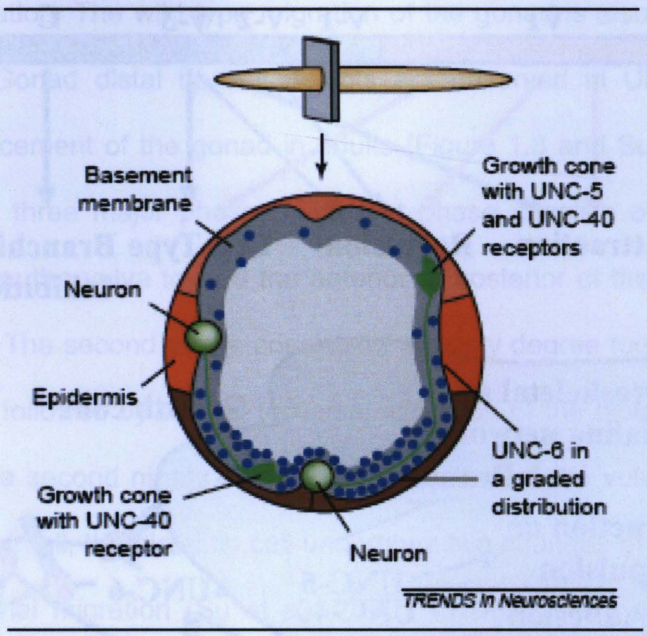

Figure 1.6: Growth cone migration and the UNC-6/netrin system

Model for the circumferential guidance of neuronal growth cones by UNC-6. A transverse section of the *C. elegans* body wall shown. Growth cones migrate along the body wall between the epidermis and basement membranes in response to a graded distribution of UNC-6 (blue), which peaks at the ventral midline. Neurons (green) expressing the UNC-5 and UNC-40 receptors migrate dorsally, while those expressing UNC-40 migrate ventrally. Adapted from Figure one of Wadsworth (2002)..

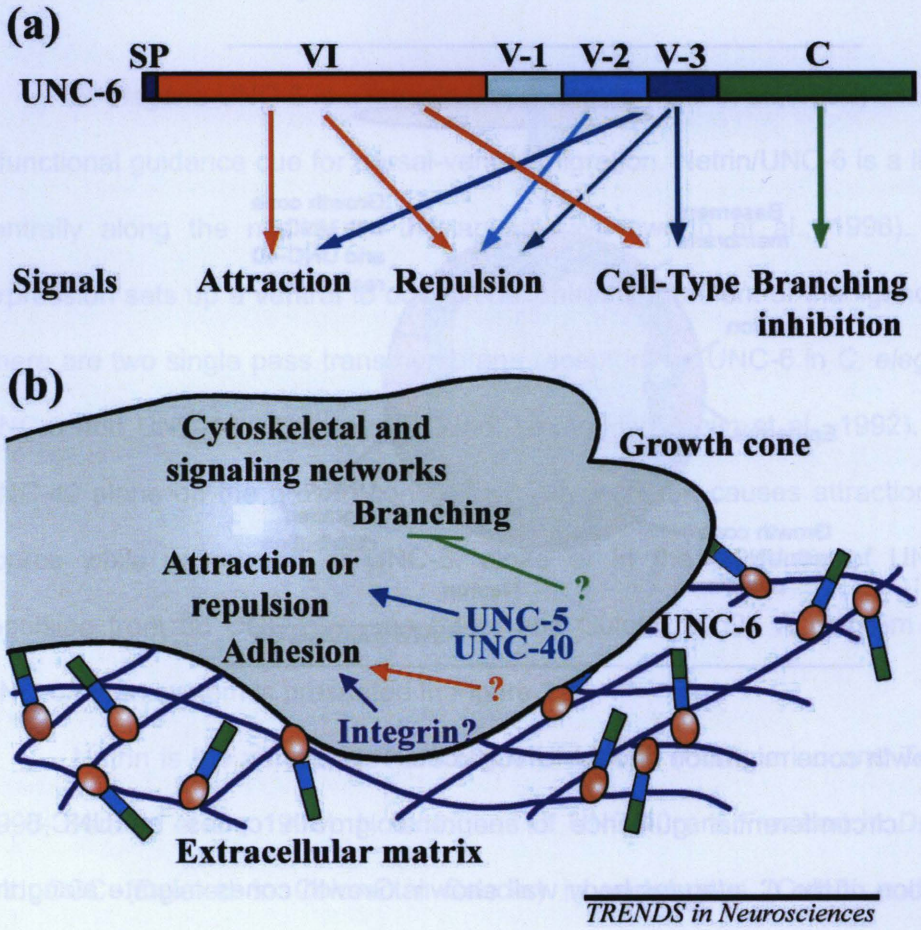

Figure 1.7: The UNC-6 ligand

(a) Domains of the UNC-6 protein: The SP domain is a typical signal peptide followed by two laminin related domains VI and V. There are three laminin-type epidermal-growth-factor-like modules labeled V-1 through V-3. The effects of each domain are denoted with arrows. (b) Model proposed by Wadsworth *et al.* in 2002 for the growth cone response of migrating axons to the extracellular guidance cue UNC-6. Integrin is suggested as a possible UNC-6 interacting partner which may be involved in adhesion. Adapted from Figure 2 of Wadsworth, 2002.

The UNC-6/netrin pathway in *C. elegans* is not exclusive to dorsal-ventral pioneer axon migration. The wild type migration of the gonad is also dependant on the UNC-6 pathway. Gonad distal tip cell defects are observed in UNC-5 null mutants leading to a displacement of the gonad in adults (Figure 1.8 and Su et al., 2000). The gonad migrates in three major phases. The first phase consists of the distal tip cell migrating away from the vulva toward the anterior or posterior of the animal depending on the gonad arm. The second phase consists of a ninety degree turn toward the dorsal side of the animal followed by ventral to dorsal migration of the distal tip cell. The third phase consists of a second ninety degree turn back toward the vulva along the dorsal side of the animal. In all, the distal tip cell undergoes two changes of direction and three periods of directional migration (Su et al., 2000). In UNC-5 null mutants, eliminating UNC-6's repulsive effects, the distal tip cell fails to make the ventral to dorsal migration of phase two resulting in a gonad which simply folds back on itself as shown in Figure 1.8. This defect is clearly visible using a dissection microscope (Hedgecock et al., 1990; Su et al., 2000; Killeen et al., 2002).

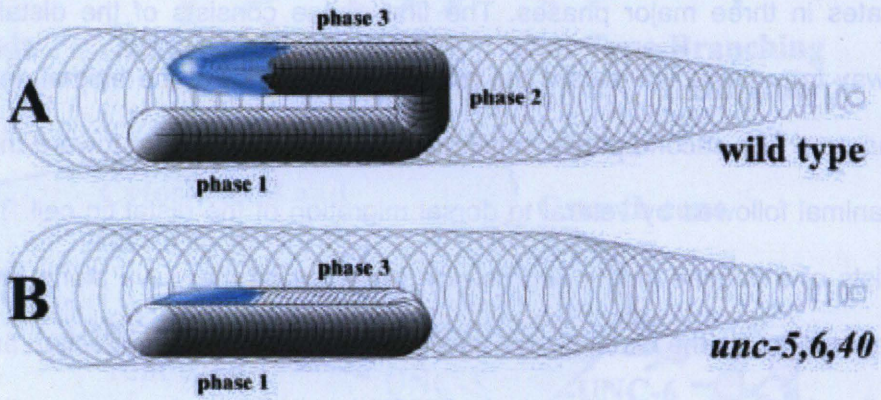

Figure 1.8: Distal tip cell migratory defects

The top cartoon (A) represents an N2 wildtype distal tip cell migration pattern resulting in a normally shaped gonad. The bottom cartoon (B) represents a netrin/UNC-6 pathway defective mutant where the distal tip cell fails to migrate dorsally and thus folds back on itself. A reproduction of Figure 2 from Su et. al. 2000.

1.5 UNC-5; a Transmembrane Receptor

The *unc-5* gene which codes for the UNC-5 protein was first described as a single pass transmembrane receptor in 1992 (Leung-Hagesteijn et al., 1992). The gene is located at +1.78 of chromosome IV. The gene product encodes a 919 amino acid protein with one helical transmembrane region (TM). The amino terminal extracellular region consists of two immunoglobulin (Ig) domains and two thrombospondin type 1 (Tsp) domains (Leung-Hagesteijn et al., 1992). Intracellularly, there is a juxta membrane domain (JM) proximal to a transmembrane domain (TM), followed by a ZD domain, a ZU-5 domain and a death domain (DD) (Killeen et al., 2002). The null allele of *unc-5* used frequently in experiments is *unc-5(e53)*. The *unc-5(e53)* null is the result of a premature stop codon mutation resulting in a peptide chain of only 283 amino acids (Killeen et al., 2002). This mutation codes for an UNC-5 protein which only codes for two Ig domains and one Tsp domain with the second Tsp domain being interrupted by the premature stop codon.

Regulation of UNC-5's cell surface expression through endocytosis is the mechanism by which a migrating growth cone is able to mediate its repulsive sensitivity to a netrin/UNC-6 source. The mechanism of UNC-5 endocytosis was elucidated in a vertebrate system. It was demonstrated that surface expression of UNC-5H1 is regulated by C-kinase-1 (PICK1) and protein kinase C (PKC) (Williams et al., 2003b). The activation PKC results in the formation of complexes of UNC-5H1/PKC/PICK which leads to the endocytosis of UNC-5H1 (Williams et al., 2003b).

Alternate splicing is an emerging field of study. Scientists are comparing mRNA sequences of the same gene and finding radical differences. In *C. elegans* no known alternate splicing of UNC-5 has been described, but in the adult rat spinal cord, the *unc-5* homologues *unc5h3* and *unc5h1* do transcribe two different forms of mRNA (Manitt et

al., 2004). Northern blot analysis of the adult rat spinal cord showed that *unc5h3* yielded two mRNA transcripts at ~12kb and ~10kb (Manitt et al., 2004). Work from the same group described the discovery through RT-PCR that *unc5h1* in adult rat spinal cord also exhibits two splice variants. They were able to sequence the mRNAs and found that the shorter of two mRNAs for *unc-5h1* lacked a second TSP domain (Manitt et al., 2004).

The UNC-5 transmembrane receptor is not solely involved in developmental guidance cue signaling; it is also involved in apoptosis as illustrated through UNC-5a knockout mice (Williams et al., 2006). Apoptosis was decreased and the number of neurons in the spinal cord was increased regardless of the presence or absence of netrin-1 in an UNC-5a knockout mouse (Williams et al., 2006). Previously the same group showed that apoptosis is a result of UNC-5a's JM region interacting with NRAGE (Williams et al., 2003a). Although interesting, the involvement of UNC-5 in apoptotic processes will not be discussed in detail.

1.6 Calcium and Netrin Signalling

Calcium levels play an integral role in netrin signaling since the concentration of Ca^{2+} can have direct effects on axon guidance. It was demonstrated that netrin signaling through interaction with DCC caused an influx of Ca^{2+} into a pioneer axon. As previously described, the result of netrin interaction with DCC on the growth cone of a migrating pioneer axon leads to migration toward the netrin source. By significantly lowering the Ca^{2+} levels within the neuron it was shown that this characteristic attraction to the netrin source could be reversed. Thus in situations of low Ca^{2+} concentration netrin signaling through DCC results in repulsion of a migrating pioneer axon away from a netrin source (Hong et al., 2000).

It has also been shown that the ratio of cAMP to cGMP has a very similar effect on pioneer axon guidance (Ming et al., 1997) leading the author of a recent review to hypothesize that the two substances are linked (Round and Stein, 2007). It is hypothesized that at high levels of cAMP to cGMP, netrin induces an attractive response through DCC by allowing Ca^{2+} to be channeled into the growth cones, while at low levels of cAMP to cGMP, Ca^{2+} is not channeled into the growth cones and a causes a repulsive response (Round and Stein, 2007).

Studies in *Xenopus* have demonstrated that transient receptor potential channels (TRPCs), which are Ca^{2+} channels, are involved in Ca^{2+} influx as a result of netrin signaling (Wang and Poo, 2005). Since PLCy activates TRPCs and netrin signalling through DCC activates PLCy a model begins to emerge. Currently, it is proposed that netrin signaling through DCC activates PLCy, and PLCy activates TRPCs, which results in the netrin induced regulation of Ca^{2+} levels in a migrating pioneer axon (Round and Stein, 2007).

Several other interesting observations have been made involving the role of Ca^{2+} in netrin signaling. Desensitization to netrin concentrations is observed with a reduction in Ca^{2+} (Ming et al., 1997). Also, signaling and transcriptional changes induced through the netrin pathway are dependant upon regulation of Ca^{2+} (Round and Stein, 2007). Much about Ca^{2+} signaling in relation to pioneer axon guidance is as of yet unknown and it will be interesting to see how future work develops our understanding of this relationship.

1.7 Downstream of UNC-6's Interaction With UNC-5

The UNC-6 receptors in *C. elegans* are relatively ambiguous in structure since their motifs do not hint at any one candidate interacting partner. However, there has

been some significant effort to elucidate the downstream members of the netrin pathway. It has been shown that tyrosine phosphorylation is required for UNC-5's function (Killeen et al., 2002) and it has been demonstrated that UNC-6 binding UNC-5 leads to UNC-5 phosphorylation in both nematodes and vertebrates (Tong et al., 2001). This was proven through disruption in UNC-5 phosphorylation leading to failure of the gene to rescue *unc-5(e53)* axon guidance defects in *C. elegans* (Killeen et al., 2002).

Investigations into these phosphorylation events have uncovered the interaction between the UNC-6 receptors and the Src family kinases. In *C. elegans* it has been demonstrated that SRC-1 interacts with UNC-5 (Lee et al., 2005) and more recently the requirement of FAK along with the Src family of kinases for the phosphorylation of UNC-5 in response to UNC-6 (Li et al., 2006). This has also been mirrored in studies in vertebrate systems (Liu et al., 2004). It has been shown that protein kinase 2 (the vertebrate homolog of FAK) is required in conjunction with the Src family kinases for the proper functioning of the netrin system (Liu et al., 2004).

Kinases are not the only proteins known to interact with UNC-5 as a result of netrin signaling. Shp2, a phosphatase, also interacts with UNC-5 (Tong et al., 2001). There are several possibilities that have been hypothesized as to the purpose of the Shp2 interaction with UNC-5. One possibility is that they are working through the mitogen activated protein kinase cascade (MAPK) which has been shown to be required for netrin mediated axon guidance (Round and Stein, 2007). Phospholipase Cy (PLCy) may be downstream of the UNC-5-Shp2 complex in the form of an inducer of endocytosis (Round and Stein, 2007). Another possibility is that PI3K is involved. PI3K is upstream of MIG10 which is involved in netrin induced lamellipodail outgrowth (Adler et al., 2006). A final possibility is that RhoA may be involved in UNC-5 function. RhoA is known to be down regulated by Shp2 and RhoA is also known to be involved, along with

guanine exchange factors, in microtubule dynamics (Round and Stein, 2007). A schematic showing a proposed downstream pathway for UNC-5 is shown in Figure 1.9.

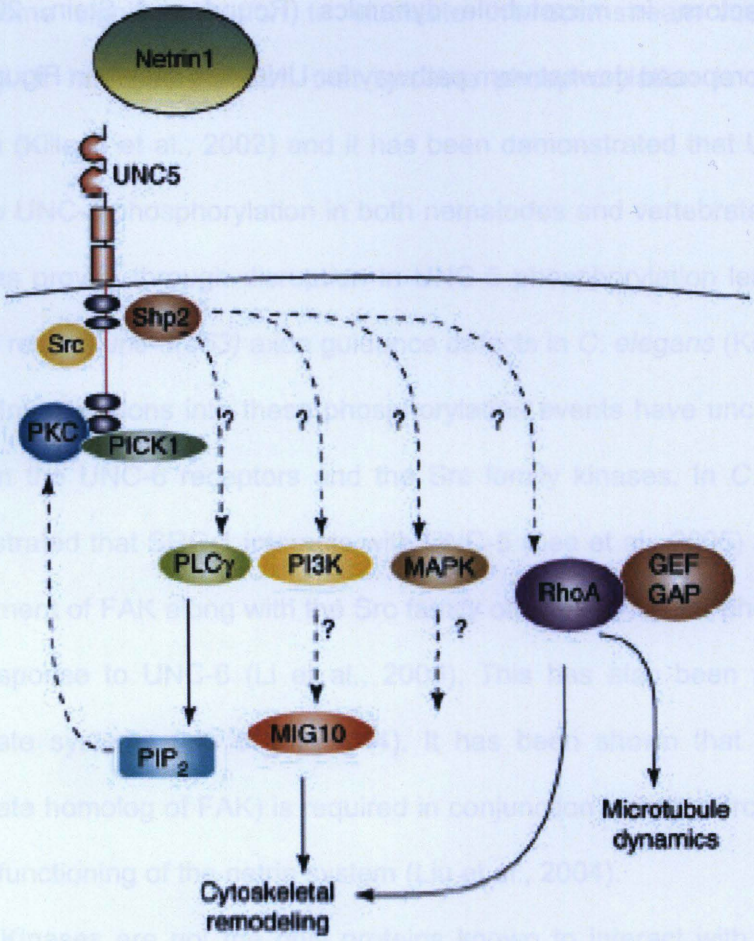

Figure 1.9: Down stream of the UNC-5 interaction with UNC-6

Image adapted from Round and Stein (2007) depicting known and hypothetical interactions with UNC-5 in a vertebrate system. Adapted from Figure 2 of Round and Stein (2007)

1.8 The *rq1* mutant strain

A commonly used technique to identify genes involved in any specific process is to screen a population of animals that have been treated with chemicals that introduce random mutations for observable defects. An enhancer screen is any screen where one aims to enhance an existing phenotype. The identification of the *rq1* mutant qualifies as an enhancer screen, since nematodes with pre-existing axon guidance defects were mutated and their progeny screened for nematodes with increased axon guidance defects. A detailed description of the discovery and subsequent analysis of the mutant *rq1* is presented in the following subsections.

1.8.1 Mutagenesis of *C. elegans* with the *unc-5* null genetic background yielded the *rq1* mutant

Mutagenesis was conducted as described in Figure 1.10. The strain used for the screen was the netrin receptor mutant, *unc-5(53)* transgenic for an integrated version of the reporter construct [*unc-129::gfp* + *dpy-20*] which allows detection of the DA and DB classes of motor neurons (Colavita et al., 1998). This strain is also known as evIS82b. Mutagenesis was performed by soaking L3-L4 animals in an ethylmethyl sulfonate (EMS) solution which is known to cause primarily G/C to A/T transition (Hope, 1999). In the F2 generation, post exposure to EMS, the mutagenized population was screened under epifluorescence for animals where the DA/DB cell bodies failed to project axons in the dorsal direction (Sybingco 2008).

As previously described, the DA/DB motor neurons have cell bodies located along the ventral cord and they project axons dorsally (White et al., 1986). These axons

normally migrate all the way from the ventral cord to the dorsal cord (Figure 1.11 A). The *unc-5(e53)* mutation causes DA/DB axon guidance defects (Hedgecock et al., 1990). The failure of the axons to successfully migrate dorsally to form the dorsal cord is a result of premature turning in the anterior posterior direction. In an *unc-5(e53)* background, despite the inability to create a functional UNC-5 transmembrane receptor, the DA/DB motor neuron cell bodies are still able to project an axon in the general dorsal direction and it is only after one to two thirds of the ventral to dorsal migration that the axons prematurely alter their migration path (Figure 1.11B). This suggests that there is some factor involved in ventral to dorsal migration of the DA/DB motor axons that is independent of UNC-5.

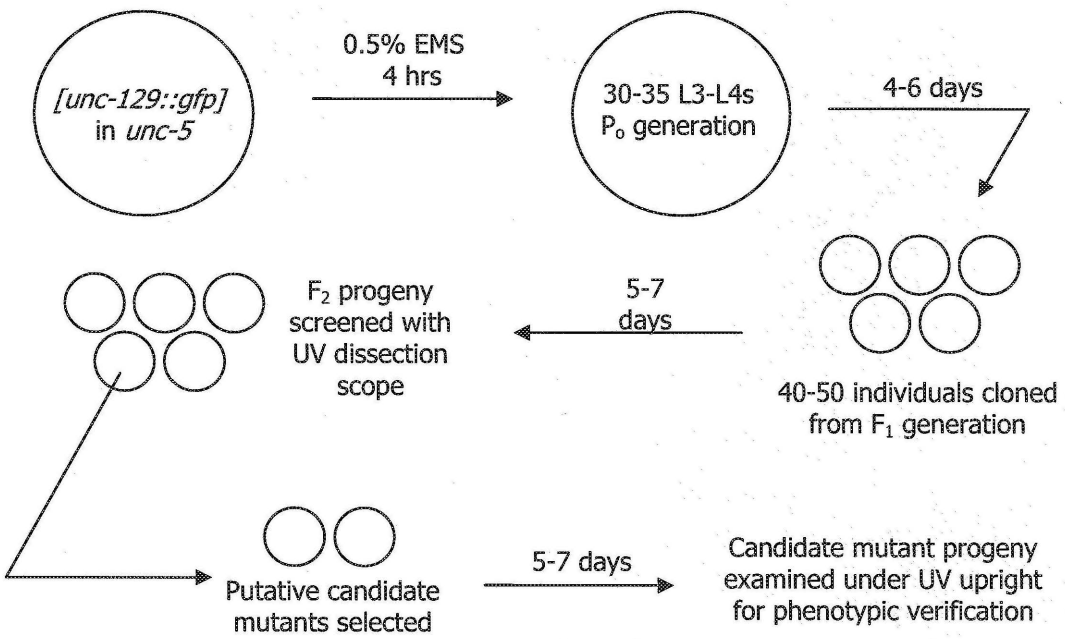

Figure 1.10: Mutagenesis and screening procedure

Animals of the *C. elegans* strain *unc-5 (e53); dpy-20 (e1282); [unc-129::gfp + dpy-20]* were bathed in a 0.5% solution of EMS for ~4 hours, and L3-L4s were selected as the parental generation. From the first generation, ~20 animals were isolated and their progeny was screened for axon guidance defects. Verification of axon guidance defects was performed under higher magnification (400-640x) after another generation.

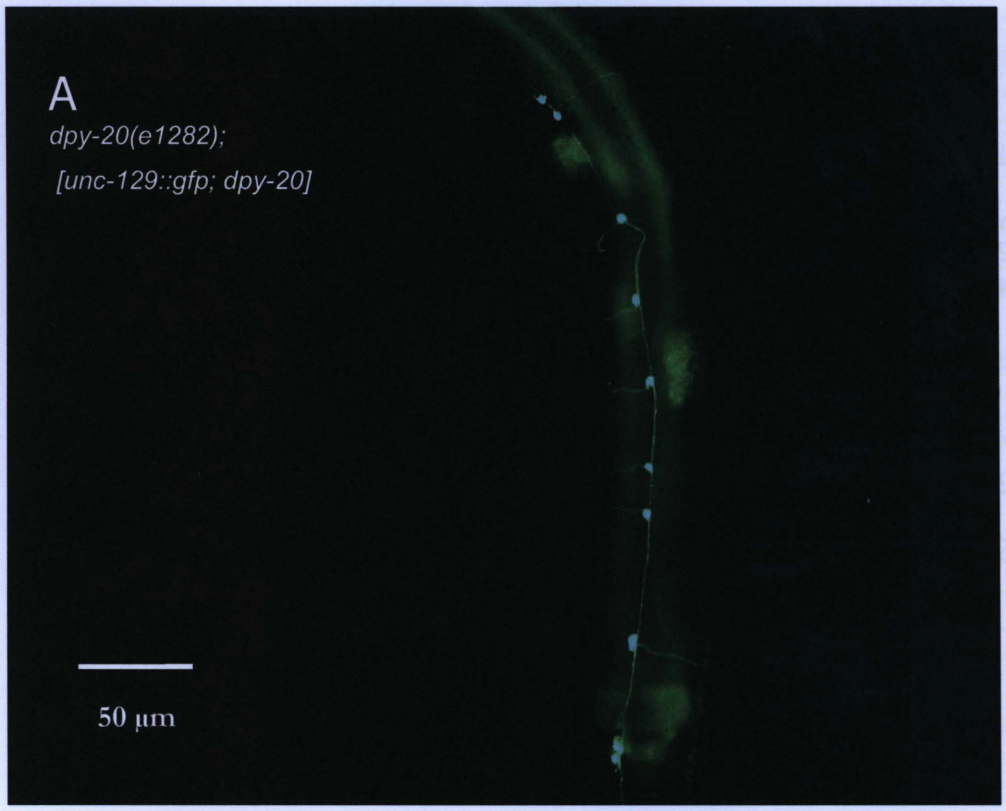

Figure 1.11: DA/DB motor axon guidance defects

A: *dpy-20 (e1282); [unc-129::gfp + dpy-20].* The ventral cord is visible displaying the DA/DB cell bodies exhibiting wild type axon outgrowth patterns. The axons migrate away from the cell bodies perpendicular to the ventral cord. *B: unc-5(e53); dpy-20 (e1282); [unc-129::gfp + dpy-20].* UNC-5 null DA/DB motor axons fail to migrate to the dorsal midline of the animal to form the dorsal cord. Despite the lack of an UNC-6 receptor to mediate repulsion from the ventral source of UNC-6 axons still consistently migrate away from the cell bodies. C: *rq1*3; unc-5(e53); dpy-20 (e1282); [unc-129::gfp + dpy-20].* The *rq1* mutant exhibits enhanced axon guidance defects in the form of cell bodies which fail to project axons in the dorsal direction (indicated by arrows).

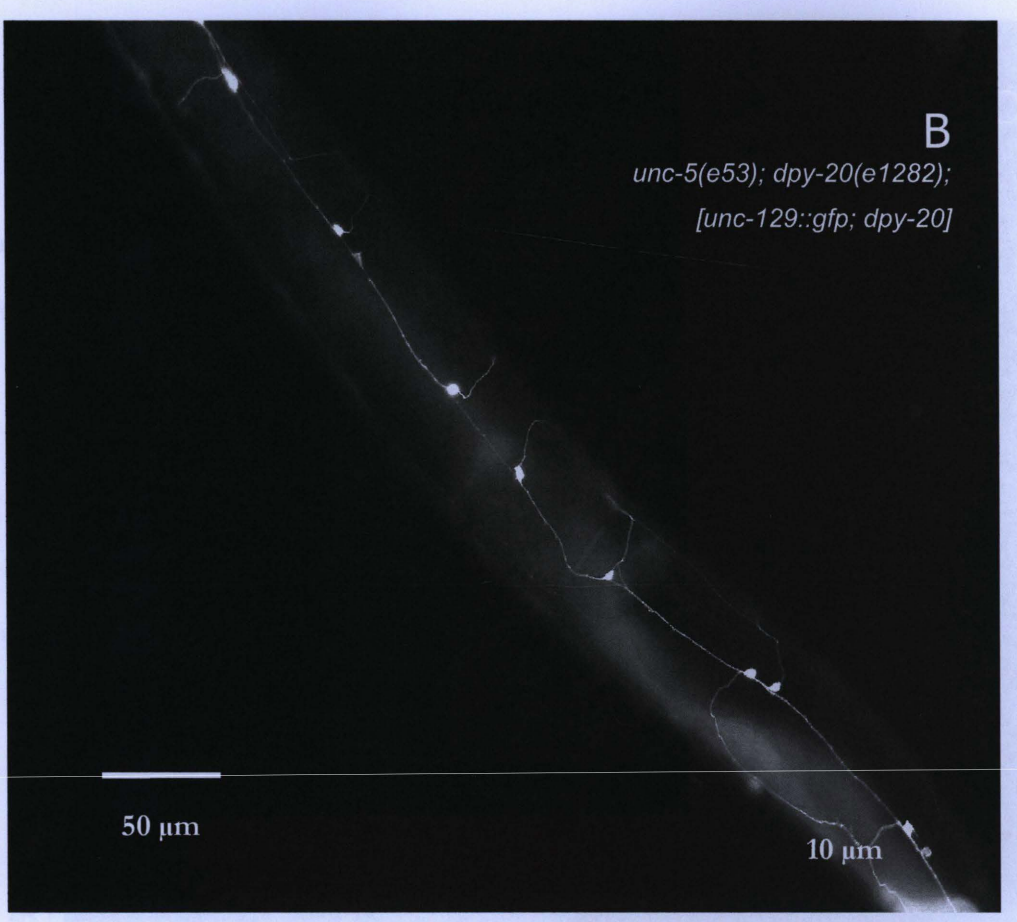
B
unc-5(e53); dpy-20(e1282);
[unc-129::gfp; dpy-20]
50 µm
10 µm

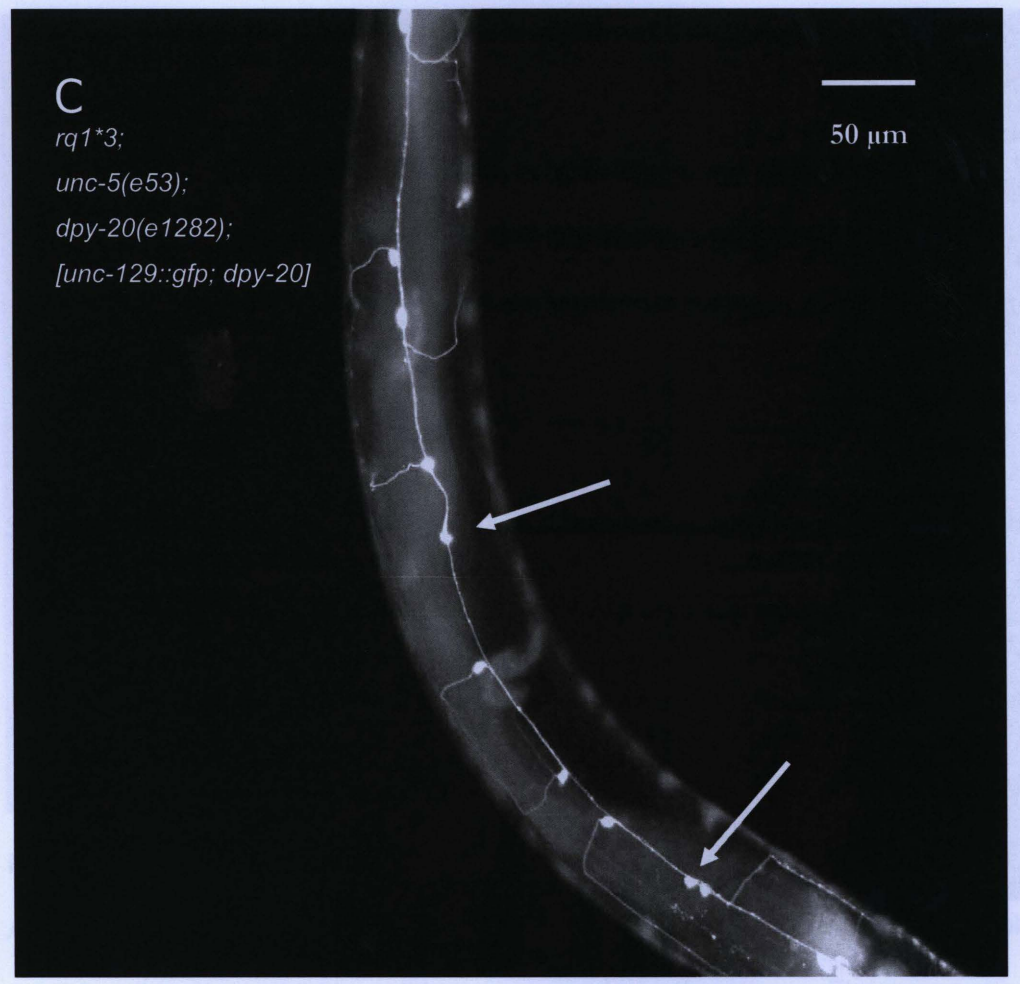
C
rq1*3;
unc-5(e53);
dpy-20(e1282);
[unc-129::gfp; dpy-20]
50 µm

1.8.2 Characterization of the *rq1* Phenotypes

Axon guidance defects. Since *rq1* was originally isolated as an enhancer of axon guidance defects of the DA and DB motor neurons, the axon guidance defects were counted and the data are presented in Figure 1.12.

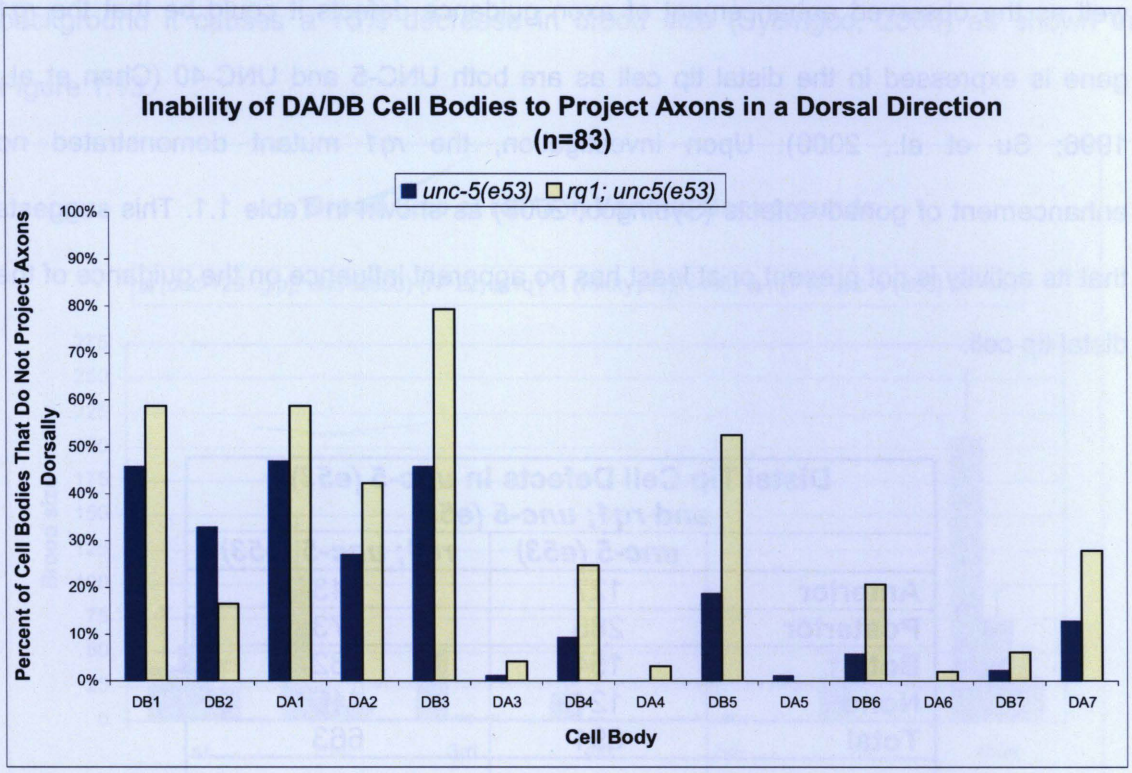

Figure 1.12: Axon guidance defects in *rq1*

The number of DA/DB cell bodies which did not project axons dorsally was scored for each cell body individually. The defects of the unc-5(e53) strain are shown in blue and of the *rq1;unc-5(e53)* double mutant are shown in yellow (Sybingco, 2008).

1.8.3. Distal Tip Cell Defects and the *rq1* Mutant

As previously mentioned, a disruption in the ability of UNC-6 to signal through UNC-5 also results in animals that display distal tip cell defects. These defects are due to the failure of the distal tip cells to migrate dorsally, causing the gonad to fold back on itself (Su et al., 2000). If the *rq1* mutation caused an enhancement in gonad defects as well as the observed enhancement of axon guidance defects it could be that the *rq1* gene is expressed in the distal tip cell as are both UNC-5 and UNC-40 (Chan et al., 1996; Su et al., 2000). Upon investigation, the *rq1* mutant demonstrated no enhancement of gonad defects (Sybingco, 2008) as shown in Table 1.1. This suggests that its activity is not present or at least has no apparent influence on the guidance of the distal tip cell.

Distal Tip Cell Defects in *unc-5 (e53)* and *rq1; unc-5 (e53)*		
	unc-5 (e53)	***rq1; unc-5 (e53)***
Anterior	127	143
Posterior	286	273
Both	154	132
None	124	115
Total	691	663
% Anterior	40.67	41.48
% Posterior	63.68	61.09

Table 1.1: Distal tip cell defects in *rq1; unc-5(e53)*

Gonad defects were observed in *unc-5(e53)* and *rq1* in an *unc-5(e53)* background. No significant difference was observed (Sybingco, 2008).

1.8.4 The *rq1* Mutant Exhibits a Low Brood Size

The *rq1* mutant was found to have another phenotype aside from the motor axon guidance defects observed in the *unc-5(e53)* background. Severe embryonic lethality was observed in both wild type and *unc-5(e53)* backgrounds. The *rq1* mutation alone causes a 50% decrease in brood size in a wild type background while in the *unc-5(e53)* background it causes a 75% decrease in brood size (Sybingco, 2008) as shown in Figure 1.13.

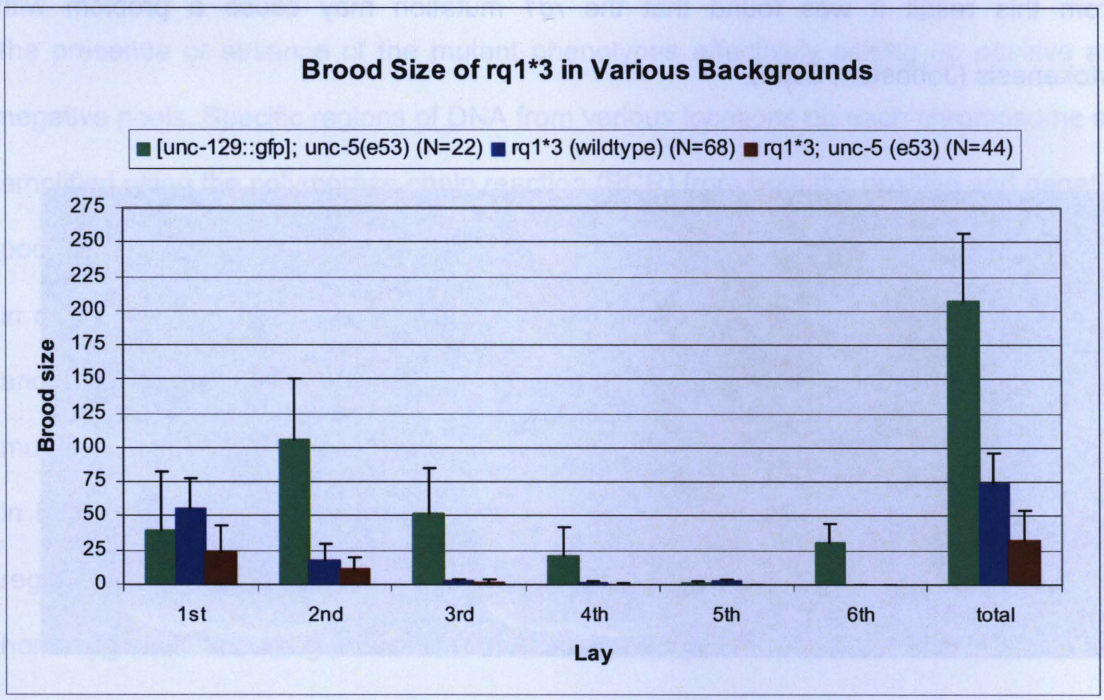

Figure 1.13: *rq1* causes reduced brood sizes

The brood sizes of the *rq1* mutant were quantified over several days. Embryonic lethality was observed in both *rq1* in an otherwise wild type and *unc-5(e53)* backgrounds with the *unc-5(e53)* background being more severe (Sybingco, 2008). The mutant *rq1* does not appear to have significant embryonic lethality so this defect is caused by *rq1*.

Preliminary investigations were performed to determine the nature of the observed embryonic lethality in *rq1*. *rq1* embryos were stained with Hoescht 33258 stain, anti-chitin and anti-wheat germ agglutinin. The chitin and Hoescht visualized images were of particular interest. A chitin shell is only present if the egg has been fertilized (Zhang et al., 2005). Hoescht staining allows the visualization of the nuclei. The wheat germ agglutinin stains the cell membrane. The chitin staining revealed that the *rq1* eggs are fertilized, however the Hoescht stain revealed irregular, diffuse nuclei. (Figure 1.14). From this result it was found that the *rq1* mutation may cause a problem with cytokenesis (Johnston, 2008).

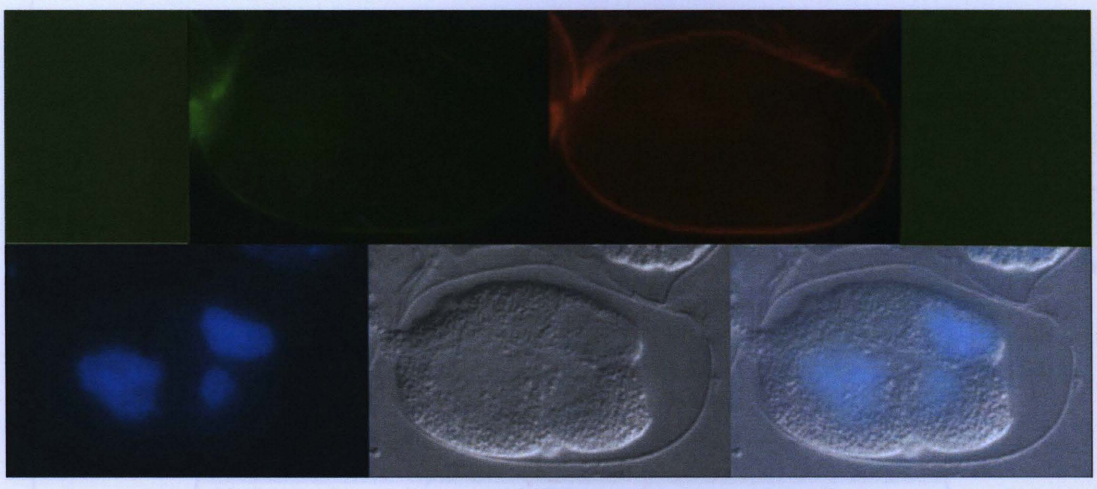

Figure 1.14: Staining of *rq1* embryos

Top row from left:visualization of wheatgerm aglutenin, visualization of chitin shell. Bottom row from left: Hoescht stain of nuclei, DIC, DIC overlay with Hoescht stain.

Staining indicates the egg is fertilized yet exhibits diffuse, irregular nuclei possibly the result of a problem with cellular division (photo produced by Dr. Johnston, 2008).

1.9 Mapping of *rq1* on the *C. elegans* genome

The mutation responsible for the phenotypes observed in the *rq1* mutant was mapped using the snip-SNP technique (Sybingco, 2008). The snip-SNP technique is named for its use of single nucleotide polymorphisms (SNPs) that interrupt restriction enzyme recognition sequences (Davis et al., 2005).

To summarize, the mutant strain in an N2 background is crossed with a wild type CB4856 strain (Hawaiian strain) and it is the differences between SNPs the two strains that makes the technique possible. The subsequent F_2 progeny are then screened for the presence or absence of the mutant phenotypes effectively setting up positive and negative pools. Specific regions of DNA from various locations on each chromosome are amplified using the polymerase chain reaction (PCR) from both the positive and negative pools. These PCR fragments contain a SNP known to interrupt a restriction enzyme site in one background but not the other. The PCR products from both pools are digested and the resultant fragments are separated on agarose gels. In regions to which the mutation is not closely linked one will observe the same heterozygous banding patterns in both pools due to the random genetic crossover in gamete formation. However, in regions to which the mutation is closely linked, the positive pool will exhibit the homozygous N2 banding patterns while the negative pool will exhibit either the Hawaiian or the heterozygous banding patterns. The homozygous N2 banding pattern is observed in the region genetically linked to the mutation since the positive pool must be homozygous for the mutation as a result of its ability to express the recessive mutant phenotype. Since the positive pool is homozygous for the mutation, it will also be homozygous for the N2 SNPs that are close to the mutation due to lack of crossing over. The snip-SNP technique is described in detail by Davis *et al.* (2005).

The *rq1* mutation was mapped to chromosome III at a genetic location of 2.126 to 3.963. This region contains 76 putative genes which consist of both known and predicted open reading frames (Sybingco, 2008).

When snip-SNP mapping had been exhausted a candidate gene approach was taken. One candidate gene was *atx-2* which was identified as a candidate gene for several reasons. As mentioned, *rq1* exhibits low brood size and embryonic lethality (Figure 1.13 and 1.14) and a previous genome-wide RNAi screen identified the *atx-2* gene as the only gene in the entire interval on chromosome III within the region where *rq1* was mapped with very early embryonic lethality of the type seen in *rq1* (Sonnichsen et al., 2005). Furthermore, its potential involvement in the nervous system made *atx-2* a prime candidate. a*tx-2* is the *C. elegans* orthologue of the human ataxin 2 gene which is known to be involved in one form of human spinocerebellar ataxia (Ciosk et al., 2004). Spinocerebellar ataxia is a dominant human progressive neurological disease somewhat similar to Huntingtons chorea.

1.10. Microinjection in *C. elegans*

Microinjection, although not technically easy, is a common method for introducing DNA into *C. elegans* (Mello et al., 1991). The technique takes advantage of the hermaphroditic nature of the reproductive system in *C. elegans.* DNA is prepared by alkaline lysis of bacterial cell lines (Birnboim and Doly, 1979) then is injected directly into the core cytoplasmic region of a young adult nematode's gonad. The distal region of the gonad consists of a sheath of unfertilized germ nuclei arrested in meiosis I surrounding a core region of cytoplasm. Importantly, the nuclei are not enclosed in a membrane and only become enveloped, along with a portion of the core cytoplasm, as they mature

toward the proximal region of the gonad (Gibert et al., 1984; Kimble and White, 1981). The concentration of DNA injected was determined to have no effect on the maximum number of transgenic F_1 animals observed, however a minimum concentration for optimal transgenic frequency was determined to be approximately 100ug/mL (Mello et al., 1991). Transgenic F_1 animals exhibited non-Mendelian patterns of inheritance which indicates that injected DNA remains extrachromosomal (Mello et al., 1991). F_2 inheritance of transgenic DNA was shown to be low and quite variable. In further experimentation it was shown that inheritance of extrachromosomal injected DNA from transgenic F_1 to transgenic F_2 was case sensitive depending on the properties of the extrachromosomal injected DNA itself (Mello et al., 1991).

1.11 RNAi in *C. elegans*

Dr. Andrew Fire and Dr. Craig Mello won the Nobel Prize in Physiology and Medicine in 2006 for their discovery of gene silencing by double-stranded ribonucleic acid (dsRNA) in *C. elegans*. The discovery was made in the mid 90s and their landmark paper was published in 1998 (Fire et al., 1998). They coined the term RNAi meaning the RNA inhibition. The method involves introduction of dsRNA into the cytosol of cells which ultimately causes the cessation of protein production at the translational stage (Parker et al., 2006).

There are three methods of introducing dsRNA into *C. elegans*. dsRNA can be directly injected into the gonad of the nematode (Fire et al., 1998), the nematodes can be bathed in a solution of dsRNA (Tabara et al., 1998) or the nematodes can be fed a bacterial strain expressing the desired dsRNA (Timmons and Fire, 1998). There are advantages and disadvantages to each technique.

The injection technique requires a small amount of dsRNA and is highly efficient, however, it is not suited to high throughput experiments since the technique is quite time consuming and requires specialized microinjection equipment. The bathing technique is suitable for high throughput experiments and screening large numbers of animals, however it requires a large quantity of purified dsRNA. The easiest technique technically is the feeding technique, however, this assumes one can create or obtain a bacterial strain expressing the desired dsRNA. Bacterial strains expressing dsRNA used to feed *C. elegans* lack the dsRNA-specific RNase-III-like endonucleases to ensure dsRNA is not degraded prior to ingestion by the nematodes (Kamath et al., 2003). While the efficiency of RNAi through the feeding method is the lowest of the three, the simplicity of the technique and adaptability to high throughput experimentation makes it the most common method of performing RNAi experiments.

The molecular mechanism of RNAi is relatively well understood. Once dsRNA is present in the cytosol of a cell, in *C. elegans,* the protein RDE-4 binds the dsRNA and, although it is not yet understood how or why, recruits the RNase III enzyme DICER (Parker et al., 2006). DICER cleaves the dsRNA into short 20~25bp segments called small interfering ribonucleic acid (siRNA) (Zamore et al., 2000). The one strand of the siRNA is called the guide strand and is incorporated into the enzyme RISC (RNA-induced silencing complex) and serves as a template for recognition of complementary mRNA (Bernstein et al., 2001). The endonuclease component of the RISC complex is Argonaute which binds the guide strand of siRNA and cleaves the complementary mRNA. This renders the mRNA useless, effectively silencing the gene from which the mRNA was transcribed (Rand et al., 2005). This method of gene silencing is highly conserved among many other species including humans.

This powerful gene silencing technique does have its limitations. For reasons unknown, RNAi does not work in all *C. elegans* tissues. In fact, the nervous

system remains relatively refractive to gene silencing through RNAi (Kamath et al., 2003). This can become a limiting factor in *C. elegans* based neurological research since direct RNAi screens can not be readily performed. Another hurdle in studies using RNAi is the residence time of proteins. Proteins that are expressed pre-RNAi treatment can have long residence times in the organism. Due to the technique targeting mRNA rather than the protein itself, complete knockout of a protein can not be assured despite inhibition efforts through RNAi (Kamath et al., 2003).

1.12 Hypothesis

The hypothesis of the work described in this thesis is that there are other molecules involved in the ventral to dorsal guidance of the DA and DB motor neurons in *C. elegans,* in addition to those in the UNC-6/netrin pathway. This can be demonstrated by finding mutants where the axon guidance defects of the strains mutant for genes in the netrin pathway are enhanced, such as *rq1* (Sybingco 2008). Once such mutants have been found, the genes must be identified. It should be determined if the mutated genes are, in fact responsible for the enhancement of the DA and DB motor axon guidance defects and whether or not they are acting within the UNC-6/netrin pathway. The first mutant for which this analysis was undertaken was *rq1* but this will be followed by the analysis of at least two other mutants isolated independently in the same screen (Sybingco 2008).

1.13 Specific objective of thesis work

The specific objective of the work described in this thesis was to locate the open reading frame and identify the gene responsible for the *rq1* phenotypes from among the 80 or so predicted genes in the interval where it was mapped (Sybingco 2008). The mutant *rq1* was identified through a genetic enhancer screen performed in an *unc-5* null background and mutants that enhanced the defects of *unc-5(e53)* were selected (Sybingco, 2008). Three such mutants were identified in the original screen, *rq1, rq2* and *rq3.* Genetic identification of *rq1* was approached using two techniques considered to be forward and reverse genetic experiments. The rescue of phenotypes was attempted using microinjection of cosmids carrying DNA derived from the region where *rq1* was mapped (Sybingco, 2008) which is considered a forward genetic experiment. The second technique, the RNAi approach, was used to inhibit mRNAs in the region where *rq1* was mapped to determine which genes recreate (phenocopy) the phenotypes of the mutant. It was expected that a mutation in a single gene would be responsible for the phenotypes observed in *rq1* since unlinked mutations were eliminated by several outcrosses of the strain with non-mutant animals (Sybingco 2008). The top candidate gene prior to these experiments was *atx-2* due to its location and involvement in cytokenesis.

2 Materials and Methods

2.1 Strains, Media and Handling of Animals

The strains used in this work were N2, LGIII: *rq1*; LG IV, *dpy-20(e1282), unc-5(e53), LGX, unc-6(ev400)*. The nematode *Caenorhabditis elegans* was grown and handled as outlined in Brenner (1974). Solid nematode growth media (NGM) was used to grow the *E. coli* strain OP50, which served as the source of nutrition for the nematodes. The OP50 strain grows to a thin lawn on NGM media due to its growth being stunted as a result of its inability to synthasize uracil (Hope, 1999). The NGM media was prepared by autoclaving 3g/L NaCl, 2.5g/L Bacto peptone, 17g/L agar followed by cooling to ~55ºC and adding 1 ml of 1M $CaCl_2$, 1ml of 1M $MgSO_4$, 25ml of 1M $KH2PO_4$ and 1ml of 5mg/ml cholesterol in ethanol per liter A 20°C incubator was used for growing all strains while manipulations were carried out at room temperature which also averaged approximately 20°C. Leica dissection microscopes were used for routine manipulations while Leica epifluorescent dissection and upright microscopes were used for screening and analysis of phenotypes. Table 2.1 lists all strains used in the experiments described.

Strain List
N2
unc-5(e53); dpy-20(e1282); [unc-129::gfp; dpy-20]
*rq1*3; dpy-20(e1282); [unc-129::gfp; dpy-20]*
*rq1*3; unc-5(e53); dpy-20(e1282); [unc-129::gfp; dpy-20]*
unc-6(ev400); dpy-20(e1282); [unc-129::gfp; dpy-20]
*rq1*3; unc-6(ev400); dpy-20(e1282); [unc-129::gfp; dpy-20]*

Table 2.1: All strains used throughout experiments

2.2 Microinjection

The *C. elegans* strains used for microinjection were the UNC-5 null strain *unc-5(e53); dpy-20(e1282) [unc129::gfp;dpy-20]* and the mutant *rq1*3;unc-5(e53); dpy-20(e1282) [unc129::gfp;dpy-20].* Cosmid clones were generously donated by the Sanger Centre in England (Table 2.2). Cosmids arrived as bacterial stabs which were streaked onto LB (10g/L tryptone, 5g/L NaCl, 5g/L yeast extract) + 10% w/v agar with 100ug/mL ampicillin and incubated overnight at 37°C. Individual colonies were picked and grown in liquid LB with 100ug/mL ampicillin and cosmid DNA isolation was performed by the alkaline lysis method (Birnboim and Doly, 1979). Fosmid clones were generously donated by the Culotti laboratory at Mount Sinai Hospital. Fosmids arrived as bacterial colonies on selective media (100ug/mL ampicillin) and fosmid DNA was also isolated using the alkaline lysis method (Birnboim and Doly, 1979). Table 2.2 lists all cosmids and fosmids used in the microinjection experiments.

Two co-injectable markers were injected, however only one was used in data acquisition. *Odr-1::gfp* is expressed in the olfactory neurons in the head of the animal (L'Etoile and Bargmann, 2000). *Odr-1::gfp* was a generous donation of Dr. Peter Roy's laboratory at the University of Toronto. This co-injectable marker was difficult to work with as it was too faint. The prefered co-injectable marker was *myo-2::yfp* which was generously donated by the Culotti laboratory at Mount Sinai Hospital. *Myo-2::yfp* DNA was transformed into DH5α *E. coli* cells which were also grown in selective media (100ug/ml ampicillin). The co-injectable marker DNA was also isolated using the alkaline lysis method (Birnboim and Doly, 1979; Sambrook et al., 1989). *Myo-2* codes for a myosin heavy chain isoform which is only expressed in the pharynx of the animal and its promoter was used to drive YFP (Miller et al., 1986). The advantage of using a *myo-*

2::yfp reporter in this experiment was the absence of any overlap between the fluorescent structures. The *myo-2::yfp* is expressed at the extreme anterior of the animal in the pharynx while the DA/DB motor neurons are located along the ventral cord of the animal with their axons being projected dorsally.

All DNA was assayed by agarose gel electrophoresis. Agarose gels were 0.7% agarose in TAE (40mM Tris, 1.0mM EDTA, adjusted to pH 8.3 with glacial acetic acid). The electrophoresis was performed at constant voltage (100V) for approximately one hour in liquid TAE buffer. Ethidium bromide (EtBr) was used to visualize the DNA under trans-ultraviolet light which was digitally photographed (Sambrook et al., 1989). The EtBr was added to the agarose gel previous to casting and solidification.

Reporter-cosmid/fosmid DNA mixture was injected at an approximate concentration of 100ng/uL from the alkaline lysis isolate with no extra treatment save for centrifugation at top speed, 14krpm in a micro-centrifuge, for ten minutes prior to injection. The injection technique was adapted from Mello *et al.*, (1991), Mello and Fire (1995). A microinjection apparatus was used obtained from Sutter Instruments. The apparatus uses compressed nitrogen gas to provide pressure to the injection system in combination with a Zeiss inverted microscope. Borosilicate glass capillaries with an internal diameter of 0.75mm were pulled to a point using P-97 Flaming/Brown Micropipette Puller (Sutter Instruments) and filled with 1.5uL of cosmid/fosmid and co-injectable marker DNA mixture. Another capillary was manually pulled to a fine rod and placed on a cover slip in Halocarbon inert oil. This filament was used to break open the tip of the pointed capillary containing the DNA under the microscope.

Injections were performed on young adult stage nematodes which were mounted on 1% agarose pads. The pads were created by drying 1% agarose in water onto Fisher brand cover slips. Injections were made directly into the distal core cytoplasm of the gonad arm at a pressure of approximately 22psi. The pressure of injection varied

inversely with the diameter of the needle. Successful injection was judged visually and based on the inflation of the distal gonad arm after injection (see Figure 2.1). Upon successful injection the nematodes were transferred to a drop of M9 solution on an NGM plate with a lawn of OP50 *E. coli*.

Cosmid List
H04D03
C38H2
M03C11
D2045
WRM0638bE04

Table 2.2: List of comids and fosmids used for microinjection

Figure 2.1: The microinjection technique

The needle is inserted into the core cytoplasm of the gonad and the arrows indicate the direction of DNA solution flow upon successful injection. Image adapted from Evans T.C. *Wormbook* (Evans, 2006)).

2.3 RNAi

The Ahringer RNAi library used had clones obtained by generous donation of Dr. Peter Roy at the University of Toronto (Fraser et al., 2000). The bacterial strain used to create the library was *E. coli HT115(DE3).* The plasmid used to create the library was pL4440. pL4440 is IPTG inducible for T7 polymerase and carries a resistance for carbenicillin.

NGM plates were used with several addititions. Carbenicillin was added at a final concentration of 25ug/mL and IPTG at a final concentration of 1mM. Bacterial library strains were grown first in liquid broth containing 50ug/mL ampicillin overnight then seeded onto the modified NGM media in 3cm diameter Petri dishes. Two *C. elegans* strains were used in this experiment: *unc-5 (e53); dpy-20 (e1282); [unc-129::gfp + dpy-20]* and *N2*.

The protocol followed was written by the Ahringer laboratory specifically for RNAi using the library they created and it is available at their website (www.gurdon.cam.ac.uk/~ahringerlab/index.html). Briefly, several L_3 nematodes were placed on the 3cm modified NGM plates seeded with the desired dsRNA expressing bacterial strain. They were incubated for three to four days until the F1 progeny have reached adulthood. The adult F_1 generation was screened microscopically for the presence of 'spoon shaped' gonad phenotype as described in section 2.4.

2.4 Analysis of Phenotypes

The F_1 progeny of the microinjected nematodes were screened for yellow fluorescence protein expression in the smooth muscle tissue of the pharynx using a Leica epifluorescent dissection microscope. Presence of the YFP-fusion protein coinjectable marker indicated the nematode was indeed transgenic at which point it was transferred to another seeded NGM plate. Once the transgenic animals had laid their first brood they were mounted onto 2% agarose in M9 buffer pads on Fisher brand glass microscope slides in a drop of M9 buffer and covered with a cover slip for observation. Nematodes were screened for the presence of outgrowing axons from DA and DB cell bodies visualized using the presence of the transgene [*unc-129::gfp* + *dpy-20*]. This transgene is also known as *evIs82B* (Colavita et al., 1998). Screening was performed using a Leica upright epifluorescent microscope using 20x, 40x and 63x objectives. The first five anterior cell bodies were omitted from the screening due to the wide range of variability. Post axonal screening, the nematodes were transferred back to a seeded NGM plate and left to recover for 3-4h prior to screening for 'spoon shaped' gonads.

Screening for 'spoon shaped' gonads was performed for both rescue of phenotypes using cosmid microinjection as well as experiments using RNAi. To dissect the gonad, nematodes were placed in a 40uL drop of 150mM KCl and 5mM HEPES solution and the heads were severed from the body by incision with an insulin needle directly behind the pharynx (as depicted in Figure 2.2). Hoescht stain 33258 (Invitrogen, SKU#H3569) was added to the liquid drop post dissection in a dark room and a cover slip was placed on the slide. Hoescht stain is used to visualize nuclei. Screening for the presence of 'spoon shaped' gonads employed the Leica upright epifluorescent microscope with the A4 ultraviolet filter at 10x, 20x and 40x objectives.

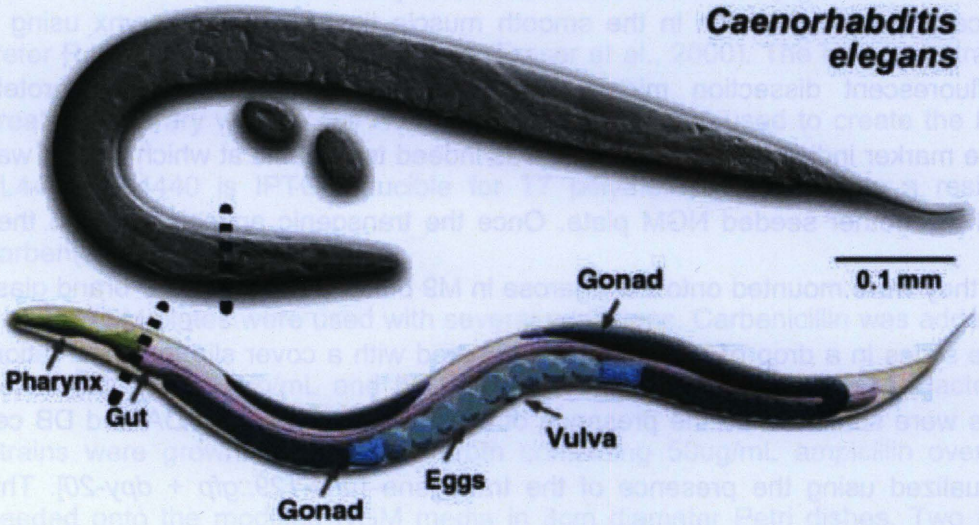

Figure 2.2: Location of incision required for gonad dissection

Adult hermaphrodite *C. elegans* are decapitated by an incision posterior of the pharynx.

3 Results

A genetic enhancer screen was conducted to identify mutants that enhanced the axon guidance defects of *unc-5(e53),* a putative null mutant lacking functional UNC-5. Three mutants were isolated, characterized and mapped on the genome (Sybingco, 2008). The three mutants were called *rq1, rq2* and *rq3.* The mutant *rq1* was determined to have mild enhancement of the axon guidance defects in an *unc-5(e53)* null mutant background and none in a wild-type background, at least in the DA and DB motor neurons (shown in Figure 1.11 and Sybingco, 2008). The *rq1* mutation was mapped to a region on chromosome III in the interval between 2.126 to 3.963 as described in the Introduction (Sybingco, 2008). This region is spanned by eight cosmids. Figure 3.1 shows the arrangement of the overlapping cosmids/fosmids in the region.

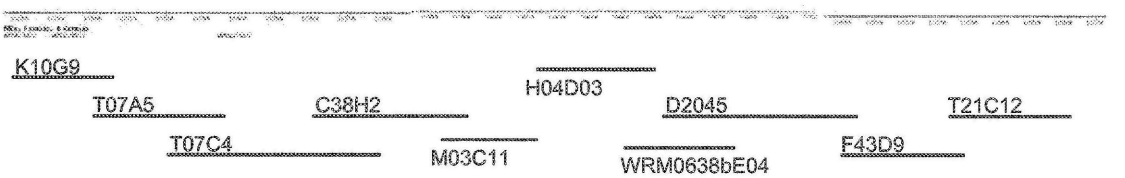

Figure 3.1: Cosmid/fosmid coverage of the region on chromosome III to which *rq1* was mapped (Wormbase; www.wormbase.org)

The 338 Kb region to which the *rq1* mutation was mapped using snip-SNP mapping and its coverage by eight cosmids (Sybingco et al., 2008). As explained in the text, the only cosmid to demonstrate rescue upon injection was H04D03.

3.1 The 'Spoon Shaped' Gonad Phenotype

The candidate gene *atx-2* was considered to be a strong candidate gene as described in the Introduction (1.11) as it was the only gene in the interval to which *rq1* was mapped that exhibited the same type of embryonic lethality as that detected in *rq1* (Sybingco 2008). Perusal of the literature indicated that when *atx-2* was knocked out using RNA inhibition, the gonads had an unusual shape, similar to a spade or spoon when they were dissected out. (Ciosk et al., 2004). Upon analysis of the *rq1* mutant gonads, it was discovered that *rq1; unc-5(e53); dpy-20(1282); [unc129::gfp+dpy-20]* exhibited a 'spoon shaped' gonad phenotype (Figure 3.2). The phenotype was also observed in *rq1* nematodes in a wild type background and an example is shown in Figure 3.2.

The penetrance of the 'spoon shaped' gonad phenotype in *rq1; unc-5(e53); dpy-20(e1282); [unc-129::gfp + dpy-20]* is approximately 30% (N=69) while *unc-5(e53); dpy-20(e1282); [unc-129::gfp + dpy-20]* exhibits less than 5% penetrance (N=58). The obvious difference between the *rq1* mutant and the background strains made this phenotype ideal for screening. This second phenotype was crucial as it provided a second quantifiable indicator of rescue through microinjection. The additional phenotypes that are also present in the mutant, such as low brood size and high incidence of males, are not suitable as indicators of rescue.

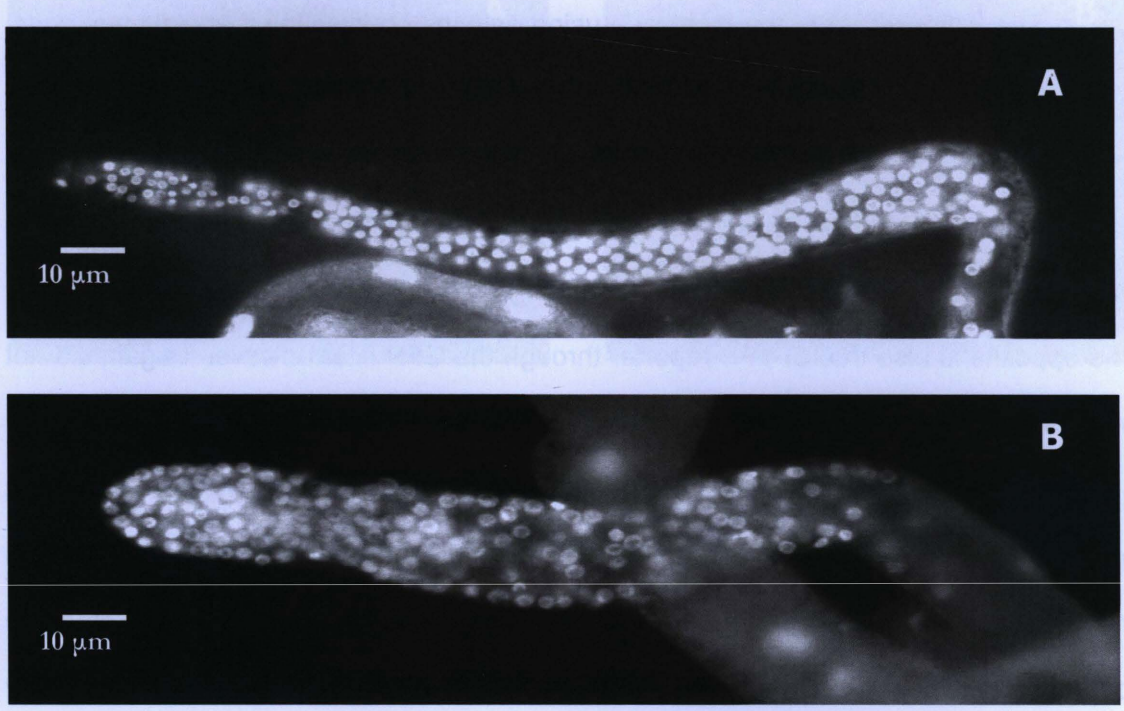

Figure 3.2: 'Spoon shaped gonad' phenotype of *rq1*

(A) Dissected gonad stained with Hoescht 33258 dye from *unc-5(e53)* (like N2) are thin and narrow distally. (B) 'Spoon shaped gonads' in *rq1*3; unc-5(e53)*, are larger with rounded, bulbous distal tips.

3.2 Rescue Of Phenotypes By Cosmid/Fosmid Microinjection

The initial set up of the technique using only the co-injection marker, *myo-2::yfp*, was successful in creating transgenic animals. Although some gut fluorescence was observed, the YFP reporter provided an excellent indication that the microinjection technique had yielded transgenic animals. The GFP neuronal reporter was faintly visible through the YFP filter however the bleed through did not significantly affect screening. The opposite is also true of YFP reporter through the GFP filter however it again did not affect screening. An example of a transgenic animal is shown in Figure 3.3.

A total of five cosmids and fosmids were injected successfully and transgenic animals were screened for both axon guidance defects and 'spoon shaped' gonads. The microinjection technique does not yield high numbers of transgenic animals. Screening for two phenotypes is tedious and time consuming due to the fact that the animals rarely survive one screening process before being subjected to the second. Also, several of the cosmids/fosmids yielded extremely low numbers of transgenic animals leading us to hypothesize that a gene present on the cosmid/fosmid was either toxic or caused the co-injection marker to be silenced. Tables 3.1 and 3.2 summarize the microinjection experiments. The only construct that showed reproducible rescue of phenotypic defects was the cosmid H04D03. The cosmid H04D03 was shown to rescue both the axon guidance defects as well as the 'spoon shaped' gonads in an *unc-5(e53)* background.

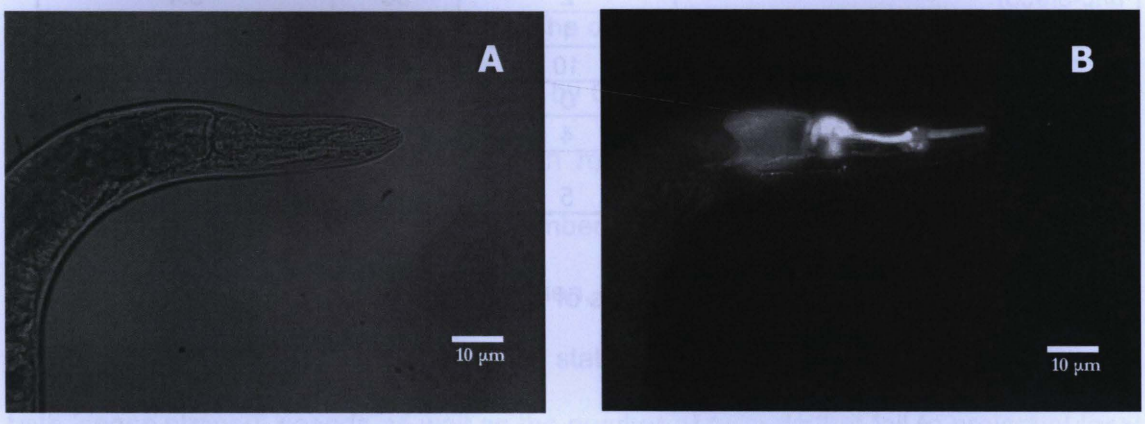

Figure 3.3: Transgenic animals expressing *myo-2::yfp*

The YFP reporter protein is expressed in the pharynx of the animal. The same transgenic animal is pictured, at left (A), with trans-white bright field microscopy and, at right (B), with epi-fluorescent microscopy.

Strain	Number Observed	N	% 'spoon shaped'
*rq1*3 in unc-5(e53)*	20	69	29.0
unc-5(e53)	2	58	3.4
*rq1*3 unc-5(e53) with* H04D03	1	24	4.2
*rq1*3 unc-5(e53) with* C38H2	10	37	27.0
*rq1*3 unc-5(e53) with* M03C11*	0	2	0.0
*rq1*3 unc-5(e53) with* D2045	4	10	40.0
*rq1*3 unc-5(e53) with* WRM0638bE04	5	13	38.5

Table 3.1: Microinjection of various strains of *C. elegans* with the cosmids indicated and screening for 'spoon shaped' gonads

All strains carry the [*unc-5::gfp* + *dpy-20*] transgene in the indicated genetic background.

* Denotes an experiment which yielded only a few transgenic animals were obtained, despite many injection attempts, presumably due to silencing of the transgene.

Strain	Number Observed	N	% With Guidance Defects
*rq1*3 in unc-5(e53)*	15	31	48.4
unc-5(e53)	7	30	23.3
*rq1*3 unc-5(e53) with* H04D03	7	25	28.0
*rq1*3 unc-5(e53) with* C38H2	10	16	62.5
*rq1*3 unc-5(e53) with* M03C11*	1	4	25.0
*rq1*3 unc-5(e53) with* D2045	7	15	46.7
*rq1*3 unc-5(e53) with* WRM0638bE04	1	2	50.0

Table 3.2: Microinjection of various *C. elegans* strains with the cosmids indicated and screening for axon guidance defects

All strains carry the [*unc-5::gfp* + *dpy-20*] transgene in the indicated genetic background.

* Denotes an experiment where only a few transgenic animals were obtained despite many injection attempts, presumably due to silencing of the transgene.

From the data presented in Tables 3.1 and 3.2, the only cosmid which caused rescue of both the axon guidance defects of DA and DB motor neurons and the 'spoon shaped' gonad phenotype was H04D03. The data from the injection of H04D03 is shown in Figures 3.4 and 3.5. Statistical analysis by Chi-squared method determined that *rq1*3* in *unc-5(e53)* is statistically different than *rq1*3* in *unc-5(e53)* with H04D03 for both 'spoon shaped' gonads as well as the number of animals that fail to project at least one DA/DB motor neuron in the dorsal direction. Also by the Chi-square method, *rq1*3* in *unc-5(e53)* with H04D03 was found to be statistically the same as *unc-5(e53)* alone for both 'spoon shaped' gonads as well as the number of animals that fail to project at least one DA/DB motor neuron in the dorsal direction. H04D03 spans a genetic region from base pairs III: 10,429,924 to base pairs 10,451,006 which is a total of 21,082 base pairs in length. As a result of microinjection alone, the region of rescue could be narrowed to five genes contained within the cosmid H04D03. These five genes are shown in Table 3.3.

The results of the microinjection experiments also yielded useful negative results as shown in Figure 3.4 and 3.5. No rescue was observed upon injection of the cosmid D2045. The D2045 cosmid overlaps with the H04D03 cosmid as shown in Figure 3.9.

Microinjection of the fosmid WRM0638bE04 also yielded negative rescue results. The region of overlap between the fosmid WRM0638bE04 and the cosmid H04D03 is much larger and partially covers the gene H04D03.3 and entirely covers the geneH04D03.4. The WRM0638bE04 coverage of the H04D03.3 gene does not include the genes promoter and only codes for the second and third of four exons.

The success of the microinjection technique was variable, despite the positive results achieved using H04D03. The technique proved to be difficult in that the ratio of the concentration of the reporter DNA to cosmid/fosmid DNA needed to be optimized for each injection despite the constant final DNA concentration remaining constant.

However, the fact that rescue of the axon guidance and the spoon shaped gonads were rescued by the H04D03 cosmid and not by several others in the region, meant that the gene mutated in *rq1* must be on this cosmid.

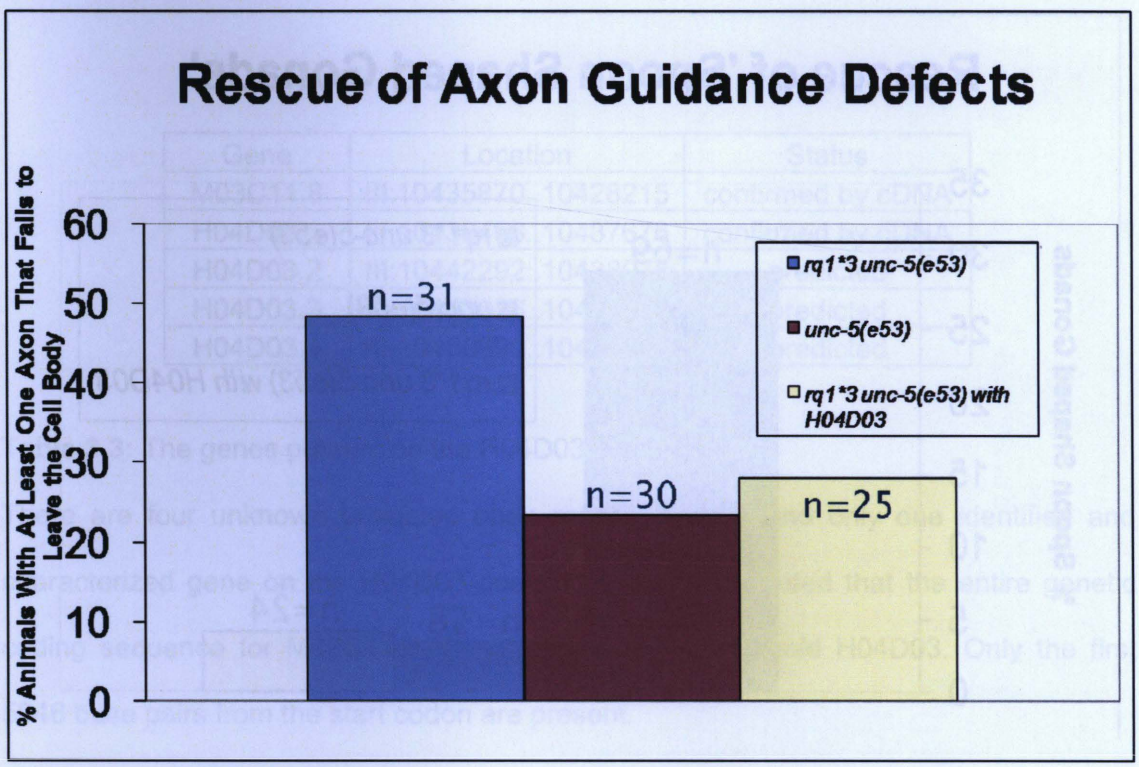

Figure 3.4: Rescue of axon guidance defects of the strain *rq1*3;unc-5(e53)[unc129::gfp + dpy-20]*

The axon guidance defects are assessed by counting the axons leaving the DA3 to DA7 cell bodies, visualized using the [*unc-129::gfp* + *dpy-20]* transgene with epifluorescent light on the upright microscope. Presented are data for the *unc-5(e53)* (blue bar) and the *rq1; unc-5(e53*) double mutant (maroon bar). The yellow bar shows the axon guidance defects for the double mutant strain that has been injected with the cosmid HO4D03 and the co-injection marker, *myo-2::yfp*.

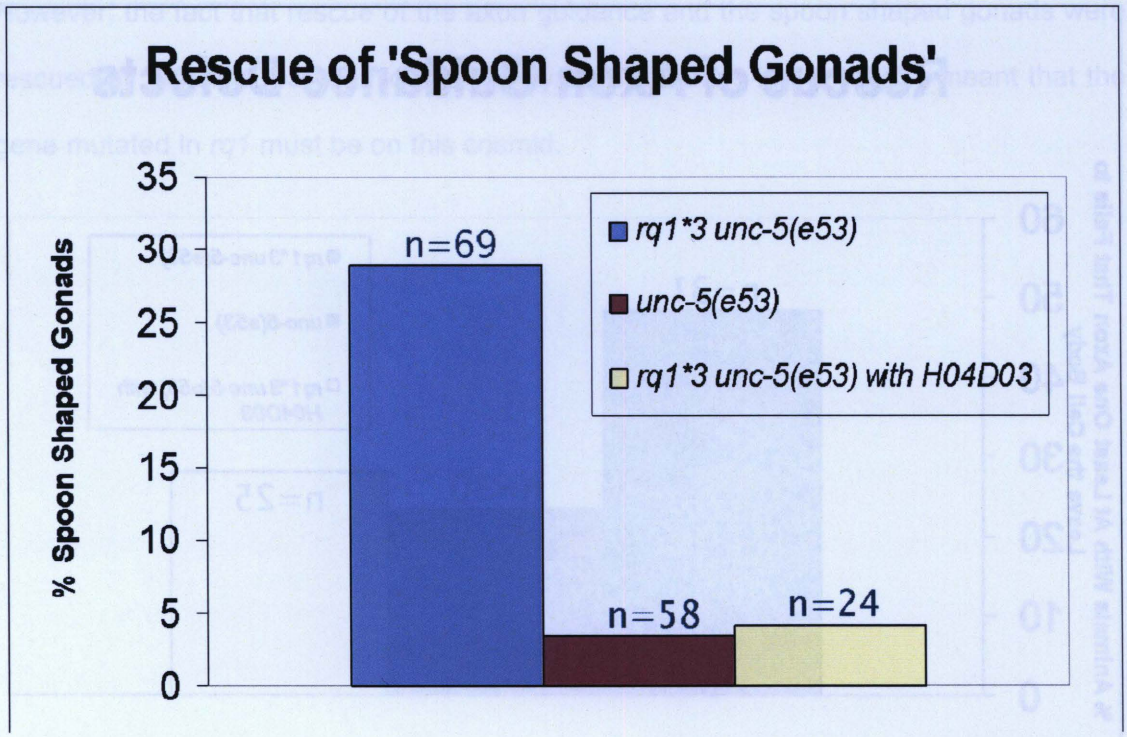

Figure 3.5 Rescue of 'spoon shaped' gonad phenotype the strain *rq1*3; unc-5(e53)[unc129::gfp + dpy-20]*

The spoon shaped gonads are assessed by dissecting out the gonads as described in Materials and Methods and staining with Hoescht 33258 dye, followed by observation with the upright microscope under epifluorescence. Presented are data for the *unc-5(e53)* (blue bar) and the *rq1; unc-5(e53)* double mutant (maroon bar). The yellow bar shows the data for the double mutant that has been injected the cosmid H03D03 along with the co-injection marker, *myo-2::yfp*.

Gene	Location	Status
M03C11.8	III:10435870..10428215	confirmed by cDNA
H04D03.1	III:10436496..10437676	confirmed by cDNA
H04D03.2	III:10442292..10438078	predicted
H04D03.3	III:10443036..10444832	predicted
H04D03.4	III:10450999..10445692	predicted

Table 3.3: The genes present on the H04D03 cosmid

There are four unknown predicted open reading frames and only one identified and characterized gene on the H04D03 cosmid. It should be noted that the entire genetic coding sequence for M03C11.8 is not present on the cosmid H04D03. Only the first 5946 base pairs from the start codon are present.

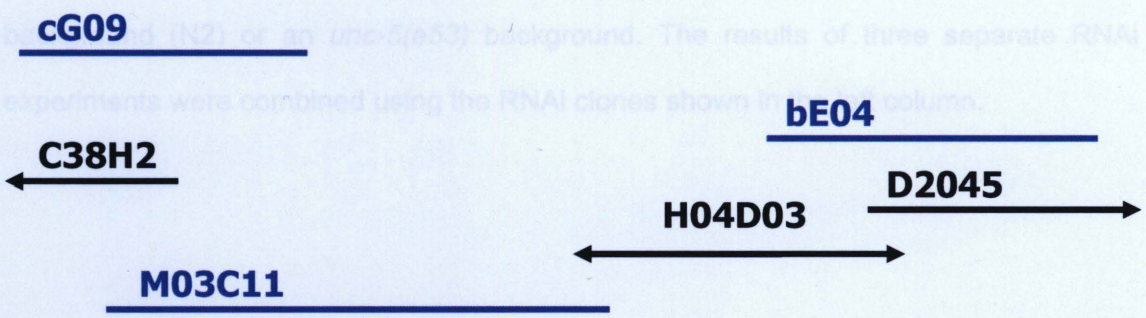

Figure 3.6: Detailed map of cosmid coverage around the cosmid H04D03

3.2. RNAi Experiments to Phenocopy the Defects of *rq1*.

RNAi was used to attempt to phenocopy the 'spoon shaped' gonad phenotype by knocking down genes known to be in the genetic region containing the *rq1* mutation. There are 18 predicted genes in the interval where *rq1* maps that are contained within the H04D03 cosmid and these are listed in Table 3.4. The results of three screens are combined in Table 3.4. The screens were performed in two backgrounds; a wild type, N2, background and an UNC-5 null background *unc-5(e53); dpy-20(e1282); [unc-129::gfp + dpy-20]* background.

One gene in the region of interest was unaccounted for in the library. H04D03.4 was not present and thus it could not be determined if a knockout of these genes causes a 'spoon shaped' gonad phenotype. The H04D03.4 gene codes for a novel predicted protein which has similarity to *zyg-11* which is known to be involved in embryonic anterior/posterior polarity (Vasudevan et al., 2007).

Gene	% Spoon Shaped Gonads			
	unc-5(e53)	N	N2	N
M03C11.2	28	36	27	36
M03C11.3	24	21	19	21
M03C11.4	0	20	21	20
M03C11.5	0	16	0	16
M03C11.6	0	12	0	12
M03C11.7	0	19	0	19
M03C11.8	41	22	0	22
H04D04.1	22	49	19	49
H04D04.2	0	18	0	18
H04D04.3	0	19	0	19
D2045.1	24	46	23	46
D2045.2	23	35	13	35
D2045.3	16	58	16	58
D2045.4	16	37	21	37
D2045.5	0	10	0	10
D2045.6	18	40	24	40
D2045.7	40	25	9	25

Table 3.4: RNAi experiments in both *unc-5(e53)* and N2 genetic backgrounds.

RNAi experiments were conducted as described in the Materials and Methods and several are capable of producing a 'spoon shaped' gonad phenotype in both a wild-type background (N2) or an *unc-5(e53)* background. The results of three separate RNAi experiments were combined using the RNAi clones shown in the left column.

3.3 Axon Guidance Defects in an *unc-6* Null Background.

Recent experiments have been ongoing to determine whether or not the *rq1* mutation is in a parallel pathway to the netrin pathway. A double mutant was created consisting of *rq1* in an *unc-6(ev400)* putative null genetic background. A comparison between the number of DA and DB motor neurons that project axons in a dorsal direction was made between the *unc-6(ev400)* null strain and an *rq1;unc-6* double mutant strain. The results are presented in Figure 3.7.

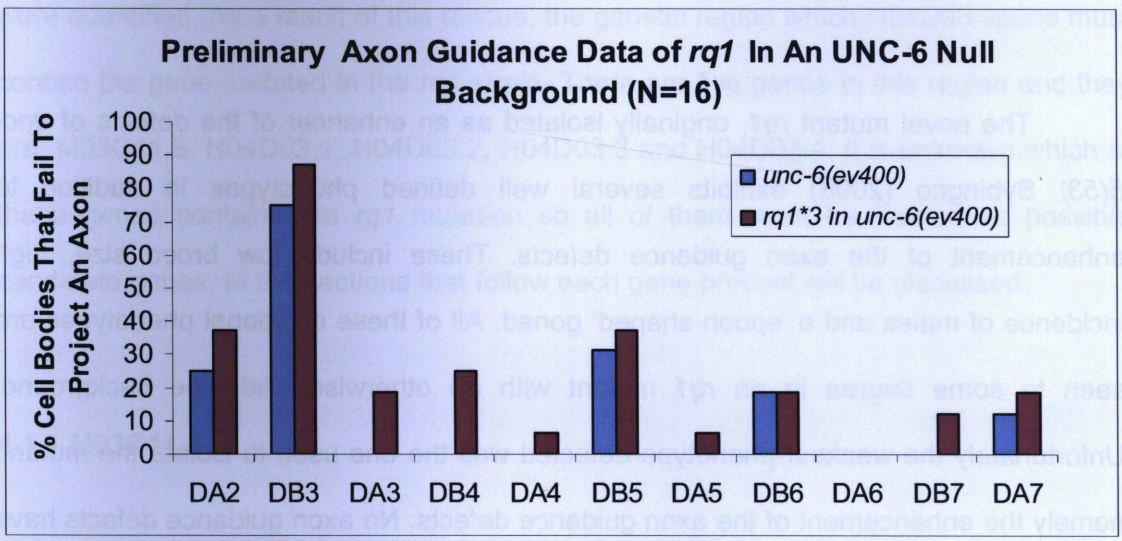

Figure 3.7: Axon guidance defects in an *rq1, unc-6(ev400)* double mutant background

The axon guidance defects are assessed by counting the axons leaving the DA3 to DA7 cell bodies, visualized using the [*unc-129::gfp* + *dpy-20]* transgene with epifluorescent light under the upright microscope. Presented are data for the *unc-6(ev4003)* (blue bar) and the *rq1; unc-6(ev400)* double mutant (maroon bar).

4 Discussion

The novel mutant *rq1,* originally isolated as an enhancer of the defects of *unc-5(53)* Sybingco (2008) exhibits several well defined phenotypes in addition to enhancement of the axon guidance defects. These include low brood size, high incidence of males and a 'spoon shaped' gonad. All of these additional phenotypes are seen to some degree in an *rq1* mutant with an otherwise wild type background. Unfortunately the weakest phenotype detected was the one used to isolate the mutant, namely the enhancement of the axon guidance defects. No axon guidance defects have been detected to date in the DA and DB motor neurons in an *rq1* mutant in an otherwise wild type background. This weak enhancement is probably due to redundancy in the pathways which guide motor neurons. Currently, investigations are underway to determine whether other neurons are affected in the mutant such as the VD and DD classes of motor neurons as well as the mechanosensory neurons or other motor neurons.

4.1 Microinjection

Microinjection with cosmid and fosmid DNA corresponding to the region where *rq1* maps was found to be successful. The technique was sensitive on a case to case basis in that each cosmid/fosmid needed to be optimized for its ratio of reporter to cosmid/fosmid DNA concentration despite the final concentration remaining approximately constant.

Despite the intricacy of the technique, transgenic animals demonstrating rescue were quantified. As a result of this rescue, the genetic region which H04D03 spans must contain the gene mutated in the *rq1* strain. There are five genes in this region and they are: M03C11.8, H04D03.1, H04D03.2, H04D03.3 and H04D03.4. It is unknown which of these genes contains the *rq1* mutation so all of them must be treated as possible candidate genes. In the sections that follow each gene product will be discussed.

4.1.1 M03C11.8

The protein M03C11.8 is a SNF2 family DNA-dependant ATPase. Although the entire coding region is not accounted for on the H04D03 cosmid it is possible that the *rq1* mutation is located in the region which is present on the cosmid. The promoter is present on the H04D03 cosmid meaning a protein, however truncated, is being expressed as a result of the presence of the cosmid. The first 5,947bp of 7,159bp of the genomic sequence is present on the cosmid which is approximately 83%. The full length protein is 989 amino acids in length and has nine exons. The H04D03 cosmid terminates near the end of the eighth exon and excludes the ninth exon.

There are twenty four known alleles of M03C11.8 gene (genetic structure shown in Figure 4.1), however, despite the fact that the identity of the gene product is known, the protein is not well characterized. The domains and their functions have all been predicted through bioinformatics. There are three predicted domains. The first is a calcium binding EF-hand which is a highly conserved active site which binds Ca2+ ions (Moncrief et al., 1990). The second is a member of the DEAD domain family of proteins and is a SNF2 family domain which is a domain found in proteins involved in several processes including transcription regulation, DNA repair, DNA replication and chromatin unwinding (Eisen et al., 1995). The third domain is a conserved helicase domain which

is known to be involved in ATP binding, helicase activity and nucleic acid binding (pfam: PF00271).

When aligning the cDNA sequences it becomes apparent that only the ninth exon is not present in the coding sequence covered by the H04D03 cosmid. BLAST alignment locates all three domains as possibly being contained within the region present on the H04D03 cosmid.

Upon performing a BLAST search, using the protein sequence a homologous protein in humans with an E value of 4.2e-142 is obtained for a protein 83.5% matching in length. This gene is SMARCAD1. SMARCAD1 is a SNF2 ATP-dependant DNA helicase (Adra et al., 2000; Raabe et al., 2001) and is the closest well documented match to the *C. elegans* M03C11.8 gene. The genetic name SMARCAD1 is an acronym for SWI/SNF-related, matrix-associated, actin-dependent regulator of chromatin, subfamily a, containing DEAD/H box 1. Mutations in SMARCAD1 are known to be involved in several diseases including tissue leiomyosarcoma, hepatocellular carcinoma, and hematologic malignancies (Adra et al., 2000). The protein itself localizes to the nucleus and is ubiquitously expressed in human tissue emphasizing its role in helicase activity (Adra et al., 2000).

In *C. elegans* there have been several large scale RNAi experiments performed. One such demonstration published by the Vidal laboratory was demonstrating the adaptation of the RNAi technique to high throughput phenome mapping (Rual et al., 2004). In this screen the gene M03C11.8 was identified as being embryonically lethal. Unfortunately this result conflicts with two, more recent, high throughput RNAi screens performed in *C. elegans*. In two separate screens performed in 2005 M03C11.8 was not identified in screens for embryonic lethality using high throughput RNAi technology (Fernandez et al., 2005; Sonnichsen et al., 2005). In our hands M03C11.8 caused the appearance of the 'spoon shaped' gonad phenotype in *unc-5(e53)* but not in N2.

A mutation in the M03C11.8 gene could shed light upon why some of the phenotypes of *rq1* are observed. DNA repair mechanisms such as that which M03C11.8 may be involved in are known to exhibit several reproducible phenotypes when they are defective. The phenotypes frequently observed as a result of DNA damage are apoptosis and a high incidence of males (O'Neil N. and Rose A., 2006), both of which are observed in *rq1*.

Despite the absence of nearly 20% of the genomic sequence the prediction that all three of the protein domains may be present makes it a valid candidate for the location of the *rq1* mutation. The assignment of the protein as a SNF2 ATP-dependant DNA helicase with homology to the human protein SMARCAD1 makes its candidacy exciting since it can be tied to oncology and apoptosis. If the *rq1* mutation is located within M03C11.8, the *rq1* mutant in *C. elegans* may become a powerful research tool in many more fields beyond developmental neurology.

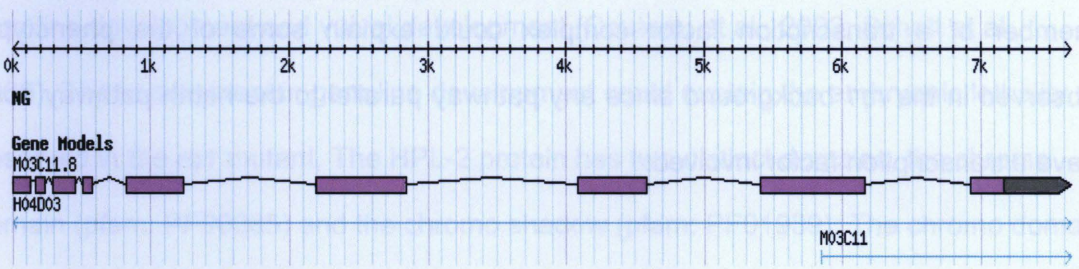

Figure 4.1: Genetic structure of M03C11.8

(WormBase http://www.wormbase.org/)

4.1.2 H04D03.1

The gene H04D03.1 encodes an unnamed protein. Very little is currently known about the protein aside from its existence. The entire gene is located within the H04D03 cosmid and, as previously stated, its removal does cause a 'spoon shaped' gonad

phenotype through RNAi experiments. The gene has three predicted exons and the protein is 204 amino acids in length (Figure 4.2). No phenotypes have been identified by high throughput RNAi screens nor have any alleles of H04D03.1 been identified.

A footnote in the http://www.wormbase.org/ file for the H04D03.1 gene indicates that the gene is similar to a *Saccharomyces cervisiae* Global transcription factor. This would prove quite interesting. However exhaustive BLAST searches have not yielded any similar results.

A pfam BLAST search did show weak homology to a membrane associating domain. The first thirty N-terminal amino acids show homology to a MARVEL domain with a high E value of 0.69. It is hypothesized that MARVEL domains could be involved in raft organization in membrane apposition events (Sanchez-Pulido et al., 2002).

Although it is an unknown gene product, it would still be exciting if the *rq1* mutation were contained within the H04D03.1 gene. The possibility of the protein being a member of a transcription factor complex could explain some of the phenotypes observed in the *rq1* background since any pathway parallel to the netrin pathway could have a transcription factor involved.

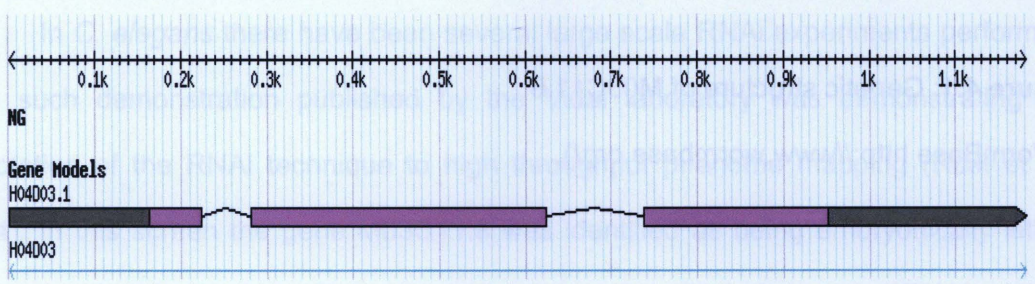

Figure 4.2: Genetic structure of H04D03.1
(WormBase, http://www.wormbase.org/)

4.1.3 H04D03.2

The gene H04D03.2 is another unnamed gene which codes for three predicted gene products, H04D03.2a, H04D03.2b and H04D03.2c, all of which are also unnamed. The first predicted gene product is predicted to be 747 amino acids in length, the second gene product is predicted to be 749 amino acids in length while the third gene product is predicted to be 92 amino acids in length (Figure 4.3).

The H04D03.2a gene product as well as the H04D03.2b gene product are both predicted to have 13 exons while the H04D03.2c gene product, being much smaller is predicted to have only two exons. All three of the gene products show homology with the *C. elegans* gene *hpl-2* at an average blast E value of 1e-41.

The *hpl-2* gene is well characterized and is also located on the third chromosome at an approximate genetic position on 5.20. It is required in several processes including germline development and vulval development (Couteau et al., 2002; Schott et al., 2006). The involvement in germline development could explain the embryonic lethality observed in the *rq1* mutant. The HPL-2 protein has two distinct domains, the chromo domain (pfam: PF00385) and the chromo shadow (pfam: PF01939). The chromo domain involved in altering the structure of chromatin (Singh et al., 1991) while the chromo shadow is a specific second chromo domain found only in heterochromatin-binding proteins (Aasland and Stewart, 1995). The homology of H04D03.2 to an important developmental protein such as HPL-2 is exciting if the *rq1* mutation maps to the H04D03.2 gene.

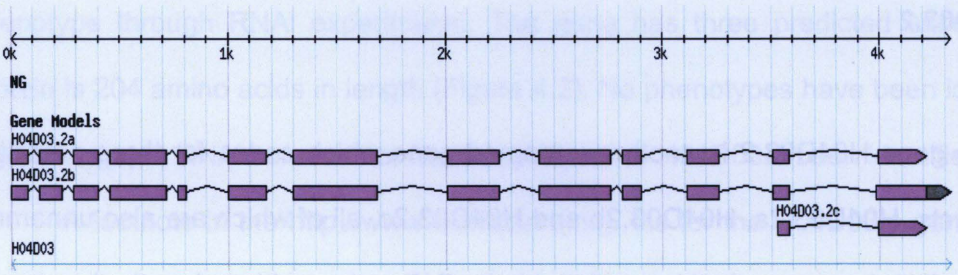

Figure 4.3: Genetic structure of H04D03.2 (a,b,c)

(WormBase, http://www.wormbase.org/)

4.1.4 H04D03.3

The gene H04D03.3 is an unnamed predicted gene. The gene product is predicted to be 409 amino acids in length and is predicted to have four exons. The protein predicted by the gene product of H04D03.3 has homology to the human ECM29 with an E value of 1.9e-12. The main functional repeat in the human protein ECM29 is a HEAT repeat (pfam: PF02985). The protein H04D03.3 has a HEAT repeat from amino acids 99-136. HEAT repeats are often present in protein phosphatases and act as protein-protein interaction sites (Groves et al., 1999). In fact, the gene product of H04D03.3 also has a phosphorylase domain from amino acid residues 339-370 (pfam:PF01048). In particular the phosphorylase domain referenced is a purine nucleoside phosphorylase however there are target differences for the same domain between species so target predictions about H04D03.3 can not be made (Mao et al., 1997).

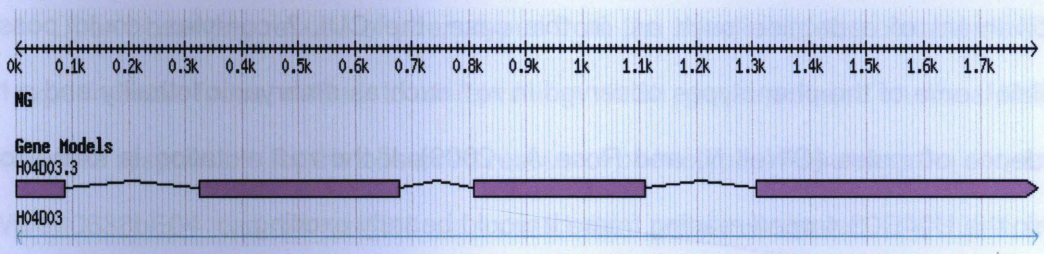

Figure 4.4: Genetic structure of H04D03.3

(WormBase, http://www.wormbase.org/)

4.1.4 H04D03.4

The gene H04D03.3 is a predicted, unnamed gene. The gene product is predicted to be 688 amino acids long coded for by eight exons. Some of this gene is also contained on the overlapping cosmid, D2045. The overlap with the D2045 cosmid is only 100bp of the first exon so no information can be gleaned about this protein from microinjection experiments with the cosmid D2045. Although the coding sequence for the gene H04D03.4 does approach the edge of the H04D03 cosmid, the open reading frame for the gene is entirely present on the cosmid.

The gene product of H04D03.4 bears homology to the human protein ZYG-11 homologue B with an E value of 1.9e-6. Upon investigation the human ZYG-11 homologue B is named for its homology to the *C. elegans* protein ZYG-11. The *C. elegans* protein ZYG-11 is a member of a CUL-2 complex (Vasudevan et al., 2007). CUL-2 complexes are involved in many developmentally crucial processes such as successful completion of meiotic anaphase II, mitotic chromosome condensation and and anterior posterior polarity in the development of the embryo (Vasudevan et al., 2007). As previously mentioned in the section discussing the candidacy of M03C11.8 the

involvement of a peptide such as, in this case, the CUL-2 complex, could possibly explain some of the phenotypes observed in *rq1* such as embryonic lethality and a high incidence of males (O'Neil N. and Rose A., 2006). If the *rq1* mutation is found to be within the H04D03.4 open reading frame it would be truly exciting.

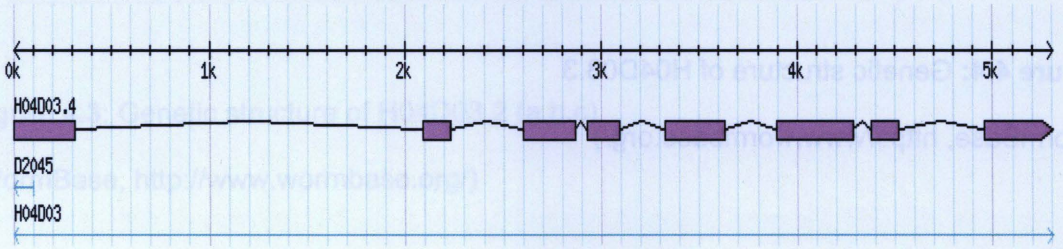

Figure 4.5: Genetic structure of H04D03.4

(WormBase, http://www.wormbase.org/)

4.1.5 Microinjection of Non-rescuing Cosmids/Fosmids

Microinjection experiments were performed using several cosmids/fosmids. Microinjecting cosmids/fosmids that do not exhibit rescue have the potential of providing conclusive results assuming the sequence of the cosmid/fosmid can be verified. Although the sequences of D2045 and WRM0638bE08 have not been verified, their results have still been presented.

The D2045 cosmid contains the genomic coding sequence for ATX-2, a candidate protein for the *rq1* mutation which upon, upon investigation, lead to the discovery of the 'spoon shaped' gonad phenotype. When injected into nematodes strains with the *rq1* mutation, no rescue is observed. This result effectively ruled out *atx-2* as a gene within which the *rq1* mutation may lie.

Upon observing rescue of phenotypes from the injection of the cosmid H04D03, the experimental focus shifted to determining which gene present on the H04D03 cosmid was responsible for the observed rescue of phenotypes. Assuming the sequence of WRM0638bE04 can be verified as correct this result eliminates H04D03.4 as a candidate gene.

4.2 RNAi Screening

The feeding method of RNAi in *C. elegans* proved successful in phenocopying the 'spoon shaped' gonad phenotype observed in the *rq1* background. It also was suited to the relatively high throughput nature of the screening that was performed. The ease of the procedure made it simple to run the RNAi experiments in parallel with other experiments despite the lengthy amounts of quantification of phenotypes required.

In total ten of the seventeen genes screened exhibited the 'spoon shaped' gonad phenotype in both the wild type background and the *unc-5(e53)* background. Although the number of genes exhibiting the phenotype was the same in both backgrounds, there were differences between the specific gene knockdowns causing the phenotype. The gene M03C11.4 exhibited 'spoon shaped' gonads in the *unc-5(e53)* background but not in the wild type background and M03C11.8 exhibited 'spoon shaped' gonads in the wild type background but not in the *unc-5(e53)* background.

Due to the nature of the RNAi mechanism a negative result from an RNAi screen such as the one performed does not provide a conclusive result. In the case of a gene knocked down by RNAi which does not demonstrate the desired phenotype one can not assume that the absence of the gene does not cause the phenotype. Some tissues and proteins with long residence times demonstrate an observed immunity to knockdown by

RNAi as observed in the nervous systems resistance to the experimental technique. In other cases, such as the RNAi data previously described, the background can become vitally important in the success of the technique. For this reason RNAi supersensitive strains have been created such as the *eri-1* strain (Kennedy et al., 2004).

4.3 Comparison of Data Sets

The RNAi screening for 'spoon shaped' gonads was successful in that it provided information about the ability of a genetic knockdown to phenocopy the 'spoon shaped' gonads observed in the *rq1* mutant. The microinjection experiment to rescue the phenotypes of the *rq1* mutant was also successful since rescue was demonstrated with the injection of the cosmid H04D03. Combining the two sets of data reveals that the observed phenotypes in *rq1* could be the result of a mutation in one of two genes. These genes are M03C11.8, H04D03.1.

The microinjection experiments revealed a possible five genes which could contain a mutation in the *rq1* strain. These genes were H04D03.1, H04D03.2, H04D03.3, H04D03.4 and M03C11.8. Microinjection has also potentially ruled out H04D03.4 as a candidate for containing the *rq1* mutation. The RNAi experiments demonstrated that when H04D3.1 and M03C11.8 were knocked down, the nematode exhibited 'spoon shaped' gonads. When the genes H04D03.2 and H04D03.3 were knocked down the nematodes did not exhibit 'spoon shaped' gonads. Unfortunately one of the only genes which were missing from the library was also located on the H04D03 cosmid and thus the gene H04D03.4 could not be assayed for 'spoon shaped' gonads in the RNAi experiment.

The combination of the RNAi data sets and the rescue of phenotypes due to microinjection experiments have empirically left two strong candidates for the identity of the gene containing the *rq1* mutation. These possibilities are the genes M03C11.8 H04D03.1 (genomic locations presented in Table 4.1). However, it should be noted that no genes located on the H04D03 cosmid can be ruled out definitively.

Gene	Genomic Location
M03C11.8	III:10435870..10428215
H04D03.1	III:10436496..10437676

Table 4.1 Best candidate genes which may contain the *rq1* mutation

The gene M03C11.8 is the only characterized gene of the three. It codes for a *C. elegans* SNF2 family DNA-dependant ATPase and has been confirmed by cDNA. The H04D03.1 gene has also been confirmed by cDNA however it is not characterized and the protein is classified as unknown.

The preliminary data presented concerning the axon guidance defects in an *unc-6* null background supports the hypothesis that *rq1* is in a parallel pathway. The data, despite the relatively low N value, indicates a clear difference between the *unc-6(ev400)* null and the *rq1; unc-6 (ev400)* double mutant. In the event that the *rq1* mutation caused a defect in a gene that is a member of the UNC-6/netrin pathway, no observed increase in axon guidance defects would be expected to be observed.

4.5 Reflections and Future Directions

The overall goal of determining what gene is altered in the *rq1* strain has the potential of being quite a lengthy process. In order to definitively prove the location of the mutation two genetic experiments have been performed. The reverse genetic approach through RNAi can yield strong positive results, however, negative results prove to be inconclusive. It is for this reason that both the forward and reverse genetic approaches must be taken together. The forward genetic approach of microinjection does provide a conclusive result assuming the sequence of the cosmid/fosmid can be positively verified. Rescue of phenotypes as a result of microinjection has conclusively demonstrated that the *rq1* mutation is located within the genetic region covered by the H04D03 cosmid.

Future experimentation to identify the precise location of the *rq1* mutation in the region covered by the H04D03 cosmid is required. The H04D03 cosmid needs to be digested into fragments containing each of its five genes, the fragments need to be purified, and each gene microinjected independently to determine which gene will cause rescue of the phenotypes.

Once the gene containing the *rq1* mutation is identified, the gene must be sequenced to identify the true nature of the *rq1* mutation. Depending on the gene identified, more experimentation will be required to understand how *rq1* is involved in nervous system development.

Double mutants need to be made between *rq1* and other known axon guidance genes such as *unc-129, unc-6* and *unc-40,* all involved in the netrin pathway. Double mutants with *slt-1* and *sax-3*, known to be involved in the Slit pathway which plays a role in ventral guidance of axons also need to be made (Hao et al., 2001). Investigations into other axons besides the DA and DB classes in *rq1* should be explored. Of particular

interest are the VD and DD classes of motor neuron which can be visualized using *unc-47::gfp* (McIntire et al., 1997) and the mechanosensory neurons which can be visualized using *mec-7::gfp* (Savage et al., 1989).

In the case that the *rq1* mutation maps to a characterized protein or a protein with known conserved domains the experiments required to determine the effects of the mutation may be performed relatively readily. If the mutation maps to a gene such as H04D03.1 where extremely little is known, more intensive work may be required. No matter which gene the *rq1* mutation maps to, several further experiments will be need to be performed. The timing and location of protein expression will need to be determined using the genes promoter to drive expression of a reporter gene. Another option is to make epitope-tagged versions of the gene to perform structure-function analysis. Finally, interacting partners can be investigated using such technologies as the yeast two hybrid method for identifying interacting partners of the *rq1* gene product.

Reflecting upon the data presented, the genes present on the H04D03 cosmid and the strong candidate genes can provide some explanations for some of the observed phenotypes in *rq1*. Of the genes for which at least some information can be attributed, it would be quite exciting if the *rq1* mutation was found to be in M03C11.8, H04D03.2 or H04D03.4. M03C11.8 is identified as a SNF2 family DNA-dependant ATPase which is involved in DNA repair. Although no direct evidence can be found to correlate the observed axon guidance defects with a SNF2 family DNA-dependant ATPase there is evidence that a SNF2 protein is downregulated prior to apoptosis suggesting downregulation of SNF2 may be an upstream trigger of apoptosis (Raabe et al., 2001). Apoptosis events have been observed in *rq1* strains and it could explain the observed embryonic lethality and possibly the high incidence of males as a result of defective DNA repair mechanisms (O'Neil N. and Rose A., 2006). A mutation in the H04D03.2 gene could partially explain the observed embryonic lethality. H04D03.2 has

homology to proteins which are known to be involved in germline development.(Couteau et al., 2002; Schott et al., 2006). H04D03.4 would also partially explain the observed embryonic lethality. H04D03.4 is similar to ZYG-11 which is a member of CUL-2 complexes which are involved in several crucial developmental events (Vasudevan et al., 2007). Defects in these developmental processes may also account for some of the observed phenotypes in *rq1*.

Shedding light on a possible parallel pathway to the *unc-6*/netrin pathway would be instrumental to expanding our understanding of nervous system development. It is my hope that the gene mutated in *rq1* is useful in many developmental and neurological studies far into the future.

5. Conclusion

Nervous system development is a complex series of events involving many as of yet not fully elucidated pathways. In order to better understand motor axon guidance mechanisms, a genetic enhancer screen was set up in the model organism *C. elegans*. A mutant, *rq1*, was identified as having increased axon guidance defects in an *unc-5(e53)* background. This mutant was also found to exhibit a low brood size and 'spoon shaped' gonads. Through the snip-SNP mapping technique the mutation was mapped to a 338Kb region on chromosome III between 2.126 and 3.963. In order to determine within which gene the *rq1* mutation lies two genetic techniques were employed, RNAi screening was employed to phenocopy the defects of the *rq1* mutant. In addition, rescue of the phenotypes of *rq1* was shown through microinjection of cosmids corresponding to the region where *rq1* had been previously mapped (Sybingco, 2008). Through these techniques the mutation has been mapped to one of five genes. From a combination of RNAi and microinjection results the best three candidate genes for containing the *rq1* mutation are M03C11.8, H04D03.1 and H04D03.4.

6 References

Aasland R,Stewart AF (1995) The chromo shadow domain, a second chromo domain in heterochromatin-binding protein 1, HP1. Nucleic Acids Res 23:3168-3173.

Ackerman SL, Kozak LP, Przyborski SA, Rund LA, Boyer BB,Knowles BB (1997) The mouse rostral cerebellar malformation gene encodes an UNC-5-like protein. Nature 386:838-842.

Adler CE, Fetter RD,Bargmann CI (2006) UNC-6/Netrin induces neuronal asymmetry and defines the site of axon formation. Nat Neurosci 9:511-518.

Adra CN, Donato JL, Badovinac R, Syed F, Kheraj R, Cai H, Moran C, Kolker MT, Turner H, Weremowicz S, Shirakawa T, Morton CC, Schnipper LE,Drews R (2000) SMARCAD1, a novel human helicase family-defining member associated with genetic instability: cloning, expression, and mapping to 4q22-q23, a band rich in breakpoints and deletion mutants involved in several human diseases. Genomics 69:162-173.

Asahina M, Valenta T, Silhankova M, Korinek V,Jindra M (2006) Crosstalk between a nuclear receptor and beta-catenin signaling decides cell fates in the C. elegans somatic gonad. Dev Cell 11:203-211.

Bernstein E, Caudy AA, Hammond SM,Hannon GJ (2001) Role for a bidentate ribonuclease in the initiation step of RNA interference. Nature 409:363-366.

Birnboim HC,Doly J (1979) A rapid alkaline extraction procedure for screening recombinant plasmid DNA. Nucleic Acids Res 7:1513-1523.

Blelloch R, Newman C,Kimble J (1999) Control of cell migration during Caenorhabditis elegans development. Curr Opin Cell Biol 11:608-613.

Brenner S (1974) The genetics of Caenorhabditis elegans. Genetics 77:71-94.

Cajal SRy (1890) Á quelle époque apparaissent les expansions des cellules nerveuses de la moëlle épiniére du poulet. Anatomomischner Anzeiger 21:609-639.

Chan SS, Zheng H, Su MW, Wilk R, Killeen MT, Hedgecock EM,Culotti JG (1996) UNC-40, a C. elegans homolog of DCC (Deleted in Colorectal Cancer), is required in motile cells responding to UNC-6 netrin cues. Cell 87:187-195.

Charron F, Stein E, Jeong J, McMahon AP,Tessier-Lavigne M (2003) The morphogen sonic hedgehog is an axonal chemoattractant that collaborates with netrin-1 in midline axon guidance. Cell 113:11-23.

Chilton JK (2006) Molecular mechanisms of axon guidance. Dev Biol 292:13-24.

Ciosk R, DePalma M,Priess JR (2004) ATX-2, the C. elegans ortholog of ataxin 2, functions in translational regulation in the germline. Development 131:4831-4841.

Colamarino SA,Tessier-Lavigne M (1995) The axonal chemoattractant netrin-1 is also a chemorepellent for trochlear motor axons. Cell 81:621-629.

Colavita A, Krishna S, Zheng H, Padgett RW,Culotti JG (1998) Pioneer axon guidance by UNC-129, a C. elegans TGF-beta. Science 281:706-709.

Couteau F, Guerry F, Muller F,Palladino F (2002) A heterochromatin protein 1 homologue in Caenorhabditis elegans acts in germline and vulval development. EMBO Rep 3:235-241.

Cramer LP (1997) Molecular mechanism of actin-dependent retrograde flow in lamellipodia of motile cells. Front Biosci 2:d260-70.

Culotti JG,Merz DC (1998) DCC and netrins. Curr Opin Cell Biol 10:609-613.

Davis MW, Hammarlund M, Harrach T, Hullett P, Olsen S,Jorgensen EM (2005) Rapid single nucleotide polymorphism mapping in C. elegans. BMC Genomics 6:118.

Eisen JA, Sweder KS,Hanawalt PC (1995) Evolution of the SNF2 family of proteins: subfamilies with distinct sequences and functions. Nucleic Acids Res 23:2715-2723.

Erskine L,Herrera E (2007) The retinal ganglion cell axon's journey: insights into molecular mechanisms of axon guidance. Dev Biol 308:1-14.

Evans TC (2006) Transformation and Microinjection. Wormbook, The C. elegans Research Community . http://www.wormbook.org/

Fernandez AG, Gunsalus KC, Huang J, Chuang LS, Ying N, Liang HL, Tang C, Schetter AJ, Zegar C, Rual JF, Hill DE, Reinke V, Vidal M,Piano F (2005) New genes with

roles in the C. elegans embryo revealed using RNAi of ovary-enriched ORFeome clones. Genome Res 15:250-259.

Fire A, Xu S, Montgomery MK, Kostas SA, Driver SE,Mello CC (1998) Potent and specific genetic interference by double-stranded RNA in Caenorhabditis elegans. Nature 391:806-811.

Fraser AG, Kamath RS, Zipperlen P, Martinez-Campos M, Sohrmann M, Ahringer J. (2000) Functional genomic analysis of C. elegans chromosome I by systematic RNA interference.Nature. 408: 325-30

Fujisawa K, Wrana JL,Culotti JG (2007) The slit receptor EVA-1 coactivates a SAX-3/Robo mediated guidance signal in C. elegans. Science 317:1934-1938.

Gibert MA, Starck J,Beguet B (1984) Role of the gonad cytoplasmic core during oogenesis of the nematode Caenorhabditis elegans. Biol Cell 50:77-85.

Gleason JE, Szyleyko EA,Eisenmann DM (2006) Multiple redundant Wnt signaling components function in two processes during C. elegans vulval development. Dev Biol 298:442-457.

Groves MR, Hanlon N, Turowski P, Hemmings BA,Barford D (1999) The structure of the protein phosphatase 2A PR65/A subunit reveals the conformation of its 15 tandemly repeated HEAT motifs. Cell 96:99-110.

Hao JC, Yu TW, Fujisawa K, Culotti JG, Gengyo-Ando K, Mitani S, Moulder G, Barstead R, Tessier-Lavigne M,Bargmann CI (2001) C. elegans slit acts in midline, dorsal-

ventral, and anterior-posterior guidance via the SAX-3/Robo receptor. Neuron 32:25-38.

Hedgecock EM, Culotti JG,Hall DH (1990) The unc-5, unc-6, and unc-40 genes guide circumferential migrations of pioneer axons and mesodermal cells on the epidermis in C. elegans. Neuron 4:61-85.

Hong K, Nishiyama M, Henley J, Tessier-Lavigne M,Poo M (2000) Calcium signalling in the guidance of nerve growth by netrin-1. Nature 403:93-98.

Hope IA, (1999) C. elegans: A Practical Approach. New York: Oxford University Press.

Huber AB, Kolodkin AL, Ginty DD,Cloutier JF (2003) Signaling at the growth cone: ligand-receptor complexes and the control of axon growth and guidance. Annu Rev Neurosci 26:509-563.

Ishii N, Wadsworth WG, Stern BD, Culotti JG,Hedgecock EM (1992) UNC-6, a laminin-related protein, guides cell and pioneer axon migrations in C. elegans. Neuron 9:873-881.

Itoh A, Miyabayashi T, Ohno M,Sakano S (1998) Cloning and expressions of three mammalian homologues of Drosophila slit suggest possible roles for Slit in the formation and maintenance of the nervous system. Brain Res Mol Brain Res 62:175-186.

Johnston W. (2008) Personal communication and provision of image.

Jorgensen EM,Mango SE (2002) The art and design of genetic screens: caenorhabditis elegans. Nat Rev Genet 3:356-369.

Kamath RS, Fraser AG, Dong Y, Poulin G, Durbin R, Gotta M, Kanapin A, Le Bot N, Moreno S, Sohrmann M, Welchman DP, Zipperlen P,Ahringer J (2003) Systematic functional analysis of the Caenorhabditis elegans genome using RNAi. Nature 421:231-237.

Kennedy S, Wang D,Ruvkun G (2004) A conserved siRNA-degrading RNase negatively regulates RNA interference in C. elegans. Nature 427:645-649.

Kidd T, Bland KS,Goodman CS (1999) Slit is the midline repellent for the robo receptor in Drosophila. Cell 96:785-794.

Killeen M, Tong J, Krizus A, Steven R, Scott I, Pawson T,Culotti J (2002) UNC-5 function requires phosphorylation of cytoplasmic tyrosine 482, but its UNC-40-independent functions also require a region between the ZU-5 and death domains. Dev Biol 251:348-366.

Kimble JE,White JG (1981) On the control of germ cell development in Caenorhabditis elegans. Dev Biol 81:208-219.

Lee J, Li W,Guan KL (2005) SRC-1 mediates UNC-5 signaling in Caenorhabditis elegans. Mol Cell Biol 25:6485-6495.

Leonardo ED, Hinck L, Masu M, Keino-Masu K, Ackerman SL,Tessier-Lavigne M (1997) Vertebrate homologues of C. elegans UNC-5 are candidate netrin receptors. Nature 386:833-838.

L'Etoile ND,Bargmann CI (2000) Olfaction and odor discrimination are mediated by the C. elegans guanylyl cyclase ODR-1. Neuron 25:575-586.

Leung-Hagesteijn C, Spence AM, Stern BD, Zhou Y, Su MW, Hedgecock EM,Culotti JG (1992) UNC-5, a transmembrane protein with immunoglobulin and thrombospondin type 1 domains, guides cell and pioneer axon migrations in C. elegans. Cell 71:289-299.

Li W, Aurandt J, Jurgensen C, Rao Y,Guan KL (2006) FAK and Src kinases are required for netrin-induced tyrosine phosphorylation of UNC5. J Cell Sci 119:47-55.

Lindwall C, Fothergill T,Richards LJ (2007) Commissure formation in the mammalian forebrain. Curr Opin Neurobiol 17:3-14.

Liu G, Beggs H, Jurgensen C, Park HT, Tang H, Gorski J, Jones KR, Reichardt LF, Wu J,Rao Y (2004) Netrin requires focal adhesion kinase and Src family kinases for axon outgrowth and attraction. Nat Neurosci 7:1222-1232.

Lu CS,Van Vactor D (2007) Synapse specificity: Wnts keep motor axons on target. Curr Biol 17:R895-8.

Manitt C, Thompson KM,Kennedy TE (2004) Developmental shift in expression of netrin receptors in the rat spinal cord: predominance of UNC-5 homologues in adulthood. J Neurosci Res 77:690-700.

Mao C, Cook WJ, Zhou M, Koszalka GW, Krenitsky TA,Ealick SE (1997) The crystal structure of Escherichia coli purine nucleoside phosphorylase: a comparison with the human enzyme reveals a conserved topology. Structure 5:1373-1383.

McIntire SL, Reimer RJ, Schuske K, Edwards RH,Jorgensen EM (1997) Identification and characterization of the vesicular GABA transporter. Nature 389:870-876.

Mello C,Fire A (1995) DNA transformation. Methods Cell Biol 48:451-482.

Mello CC, Kramer JM, Stinchcomb D,Ambros V (1991) Efficient gene transfer in C.elegans: extrachromosomal maintenance and integration of transforming sequences. EMBO J 10:3959-3970.

Merz DC,Culotti JG (2000) Genetic analysis of growth cone migrations in Caenorhabditis elegans. J Neurobiol 44:281-288.

Miller DM, Stockdale FE,Karn J (1986) Immunological identification of the genes encoding the four myosin heavy chain isoforms of Caenorhabditis elegans. Proc Natl Acad Sci U S A 83:2305-2309.

Ming GL, Song HJ, Berninger B, Holt CE, Tessier-Lavigne M,Poo MM (1997) cAMP-dependent growth cone guidance by netrin-1. Neuron 19:1225-1235.

Moncrief ND, Kretsinger RH,Goodman M (1990) Evolution of EF-hand calcium-modulated proteins. I. Relationships based on amino acid sequences. J Mol Evol 30:522-562.

Moore SW, Tessier-Lavigne M,Kennedy TE (2007) Netrins and their receptors. Adv Exp Med Biol 621:17-31.

O'Neil N., Rose A., (2006) DNA Repair. In: Worm Book, Creative Commons Attribution License.

Pan CL, Howell JE, Clark SG, Hilliard M, Cordes S, Bargmann CI,Garriga G (2006) Multiple Wnts and frizzled receptors regulate anteriorly directed cell and growth cone migrations in Caenorhabditis elegans. Dev Cell 10:367-377.

Parker GS, Eckert DM,Bass BL (2006) RDE-4 preferentially binds long dsRNA and its dimerization is necessary for cleavage of dsRNA to siRNA. RNA 12:807-818.

Raabe EH, Abdurrahman L, Behbehani G,Arceci RJ (2001) An SNF2 factor involved in mammalian development and cellular proliferation. Dev Dyn 221:92-105.

Rand TA, Petersen S, Du F,Wang X (2005) Argonaute2 cleaves the anti-guide strand of siRNA during RISC activation. Cell 123:621-629.

Riddle DL, Blumenthal T, Meyer BJ, Priess JR, (1997) C elegans II. Ney York: Cold Spring Harbour Laboratory Press.

Rothberg JM, Hartley DA, Walther Z,Artavanis-Tsakonas S (1988) slit: an EGF-homologous locus of D. melanogaster involved in the development of the embryonic central nervous system. Cell 55:1047-1059.

Round J,Stein E (2007) Netrin signaling leading to directed growth cone steering. Curr Opin Neurobiol 17:15-21.

Rual JF, Ceron J, Koreth J, Hao T, Nicot AS, Hirozane-Kishikawa T, Vandenhaute J, Orkin SH, Hill DE, van den Heuvel S,Vidal M (2004) Toward improving Caenorhabditis elegans phenome mapping with an ORFeome-based RNAi library. Genome Res 14:2162-2168.

Sambrook J, Fritsch EF, Maniatis T, (1989) Molecular Cloning: A Laboratory Manual New York: Cold Spring Harbour Press.

Sanchez-Pulido L, Martin-Belmonte F, Valencia A,Alonso MA (2002) MARVEL: a conserved domain involved in membrane apposition events. Trends Biochem Sci 27:599-601.

Savage C, Hamelin M, Culotti JG, Coulson A, Albertson DG,Chalfie M (1989) mec-7 is a beta-tubulin gene required for the production of 15-protofilament microtubules in Caenorhabditis elegans. Genes Dev 3:870-881.

Schott S, Coustham V, Simonet T, Bedet C,Palladino F (2006) Unique and redundant functions of C. elegans HP1 proteins in post-embryonic development. Dev Biol 298:176-187.

Serafini T, Colamarino SA, Leonardo ED, Wang H, Beddington R, Skarnes WC,Tessier-Lavigne M (1996) Netrin-1 is required for commissural axon guidance in the developing vertebrate nervous system. Cell 87:1001-1014.

Singh PB, Miller JR, Pearce J, Kothary R, Burton RD, Paro R, James TC,Gaunt SJ (1991) A sequence motif found in a Drosophila heterochromatin protein is conserved in animals and plants. Nucleic Acids Res 19:789-794.

Sonnichsen B, Koski LB, Walsh A, Marschall P, Neumann B, Brehm M, Alleaume AM, Artelt J, Bettencourt P, Cassin E, Hewitson M, Holz C, Khan M, Lazik S, Martin C, Nitzsche B, Ruer M, Stamford J, Winzi M, Heinkel R, Roder M, Finell J, Hantsch H, Jones SJ, Jones M, Piano F, Gunsalus KC, Oegema K, Gonczy P, Coulson A, Hyman AA,Echeverri CJ (2005) Full-genome RNAi profiling of early embryogenesis in Caenorhabditis elegans. Nature 434:462-469.

Su M, Merz DC, Killeen MT, Zhou Y, Zheng H, Kramer JM, Hedgecock EM,Culotti JG (2000) Regulation of the UNC-5 netrin receptor initiates the first reorientation of migrating distal tip cells in Caenorhabditis elegans. Development 127:585-594.

Sybingco S (2008) Identification and analysis of novel mutants exhibiting defects in pioneer axon guidance in *C. elegans*. Masters thesis, York University Library, Toronto.

Tabara H, Grishok A,Mello CC (1998) RNAi in C. elegans: soaking in the genome sequence. Science 282:430-431.

Timmons L,Fire A (1998) Specific interference by ingested dsRNA. Nature 395:854.

Tong J, Killeen M, Steven R, Binns KL, Culotti J,Pawson T (2001) Netrin stimulates tyrosine phosphorylation of the UNC-5 family of netrin receptors and induces Shp2 binding to the RCM cytodomain. J Biol Chem 276:40917-40925.

Vasudevan S, Starostina NG,Kipreos ET (2007) The Caenorhabditis elegans cell-cycle regulator ZYG-11 defines a conserved family of CUL-2 complex components. EMBO Rep 8:279-286.

Wadsworth WG (2002) Moving around in a worm: netrin UNC-6 and circumferential axon guidance in C. elegans. Trends Neurosci 25:423-429.

Wadsworth WG, Bhatt H,Hedgecock EM (1996) Neuroglia and pioneer neurons express UNC-6 to provide global and local netrin cues for guiding migrations in C. elegans. Neuron 16:35-46.

Wang GX,Poo MM (2005) Requirement of TRPC channels in netrin-1-induced chemotropic turning of nerve growth cones. Nature 434:898-904.

White J, Southgate E, Thomson J,Brenner S (1986) The structure of the nervous system of the nematode *Caenorhabditis elegans*. Phil Trans Royal Soc London B:1-340.

Williams ME, Lu X, McKenna WL, Washington R, Boyette A, Strickland P, Dillon A, Kaprielian Z, Tessier-Lavigne M,Hinck L (2006) UNC5A promotes neuronal apoptosis during spinal cord development independent of netrin-1. Nat Neurosci 9:996-998.

Williams ME, Strickland P, Watanabe K,Hinck L (2003a) UNC5H1 induces apoptosis via its juxtamembrane region through an interaction with NRAGE. J Biol Chem 278:17483-17490.

Williams ME, Wu SC, McKenna WL,Hinck L (2003b) Surface expression of the netrin receptor UNC5H1 is regulated through a protein kinase C-interacting protein/protein kinase-dependent mechanism. J Neurosci 23:11279-11288.

Yu TW,Bargmann CI (2001) Dynamic regulation of axon guidance. Nat Neurosci 4 Suppl:1169-1176.

Zamore PD, Tuschl T, Sharp PA,Bartel DP (2000) RNAi: double-stranded RNA directs the ATP-dependent cleavage of mRNA at 21 to 23 nucleotide intervals. Cell 101:25-33.

Zhang Y, Foster JM, Nelson LS, Ma D,Carlow CK (2005) The chitin synthase genes chs-1 and chs-2 are essential for C. elegans development and responsible for chitin deposition in the eggshell and pharynx, respectively. Dev Biol 285:330-339.